Cultivation and characterization of E. coli protein – secretion strains

Jurić, Laura

prehrambeno biotehnološki fakultet

zir.nsk.hr

dabar
DIGITALNI AKADEMSKI ARHIVI I REPOZITORIJI

UNIVERSITY OF ZAGREB

FACULTY OF FOOD TECHNOLOGY AND BIOTECHNOLOGY

GRADUATE THESIS

Zagreb, July 2018.   Laura Jurić

677 / BPI

CULTIVATION AND CHARACTERIZATION OF *E. coli* PROTEIN – SECRETION STRAINS

ACKNOWLEDGEMENTS

UZGOJ I KARAKTERIZACIJA *E. coli* PROTEIN – SEKRECIJSKIH SOJEVA

Laura Jurić, 677 / BPI

Sažetak: *Escherichia coli* je jedan od najčešće korištenih mikroorganizama za proizvodnju rekombinantnih proteina. Veliku većinu proteina proizvodi intracelularno, bilo u citoplazmi ili u periplazmi, tako da dobivanje biološki aktivnih proteina predstavlja izazov. Ekstracelularnom proizvodnjom proteina izbjeglo bi se mehaničko razbijanje stanica, olakšala izolacija i pročišćavanje proteina. Jedan od pristupa, primjenjen i istražen u ovome radu, je upotreba takozvanih *leaky* mutanata. Zbog mutacija u genima koji kodiraju za proteine stanične stijenke, ovi mutanti bi trebali pokazivati povećanu sposobnost izlučivanja proteina iz periplazme u hranjivu podlogu nakon translokacije proteina prirodno prisutnim bakterijskim translokacijskim mehanizmima. Dva *knock-out* soja bakterije *E. coli* su kultivirani najprije u tikvicama (bez i s pAppA plazmidom) a zatim i u bioreaktorima. Kultivirani sojevi su karakterizirani obzirom na rast, koncentraciju proizvedenog proteina i sposobnost sekrecije koristeći fitazu kao *reporter* protein.

Ključne riječi: *E. coli*, stanična stijenka, sekrecija proteina, *leaky* mutanti, fitaza

Rad sadrži: 79 stranica, 40 slika, 17 tablica, 38 literaturnih navoda, 2 priloga

Jezik izvornika: engleski

Rad je u tiskanom i elektroničkom (pdf format) obliku pohranjen u: Knjižnica Prehrambeno-biotehnološkog fakulteta, Kačićeva 23, Zagreb

Mentor na Prehrambeno-biotehnološkom fakultetu: prof. dr. sc. Božidar Šantek

Neposredni voditelj: prof. dr. sc. Karl Friehs

Pomoć pri izradi: Gabriele Kleiner-Grote, mag. ing.

Stručno povjerenstvo za ocjenu i obranu:
1. Prof.dr.sc. Blaženka Kos
2. Prof.dr.sc. Božidar Šantek
3. Izv.prof.dr.sc. Tonči Rezić
4. Doc.dr.sc. Andreja Leboš - Pavunc (zamjena)

Datum obrane: 13. srpnja 2018.

BASIC DOCUMENTATION CARD

University of Zagreb
Faculty of Food Technology and Biotechnology
Department of Biochemical Engineering
Laboratory for Biochemical Engineering, Industrial Microbiology and Malting and Brewing Technology
Scientific area: Biotechnical Sciences
Scientific field: Biotechnology

CULTIVATION AND CHARACTERIZATION OF *E. coli* PROTEIN – SECRETION STRAINS

Laura Jurić, 677 / BPI

Abstract: *Escherichia coli* is one of the most commonly used microorganisms for production of recombinant proteins. The vast majority of proteins are produced intracellular, either in cytoplasm or periplasm, so that obtaining a biologically active proteins represents a challenge. With extracellular production of proteins, would be avoided cell disruption, ease protein yielding and purification. One of the approaches, applied and investigated in this thesis, is using so-called *leaky* mutants. Due to mutations in genes encoding for proteins of the cell membrane, these mutants show an increased protein release from periplasm to nutrient medium after protein has been translocated by using natural bacterial translocation systems. Two *E. coli knock-out* strains have been cultivated first in flasks (without and with pAppA plasmid) and then in bioreactors. Strains have been characterized regarding to their growth, protein production and secretion ability, using phytase as *reporter* protein.

Keywords: *E. coli*, cell wall, secretion, *leaky* mutants, phytase

Thesis contains: 79 pages, 40 figures, 17 tables, 38 references, 2 supplements

Original in: English

Graduate Thesis in printed and electronic (pdf format) version is deposited in: Library of the

Faculty of Food Technology and Biotechnology, Kačićeva 23, Zagreb.

Mentor at Faculty of Food Technology and Biotechnology: Božidar Šantek, PhD, Full professor

Principal investigator: Karl Friehs, PhD, Prof.

Technical support and assistance: Gabriele Kleiner-Grote, M. Sc.

Reviewers:
1. Blaženka Kos, PhD., Full professor
2. Božidar Šantek, PhD., Full professor
3. Tonči Rezić, PhD., Associate professor
4. Andreja Leboš - Pavunc, PhD., Assistant professor (substitute)

Thesis defended: 13 July 2018

TABLE OF CONTENTS

1. **INTRODUCTION**

The bacterium *Escherichia coli* is one of the most commonly used hosts for producing recombinant proteins. Despite several advantageous characteristics like simplicity, safety, short doubling time, simple genetic manipulation, high protein yields and easy cultivation in common nutrient media, inadequate secretion to the extracellular environment represents a severe drawback for industrial production processes. *E. coli* belongs to a group of Gram-negative bacterium, so that its cell envelope comprises two membranes – the inner cytoplasmic membrane and the outer membrane. Besides providing protection for the cell and structural integrity, the cell envelope represents a bottleneck in extracellular production of recombinant proteins. The vast majority of proteins are produced intracellular, either in cytoplasm or periplasm, so that the downstream processing represents a challenging task in order to obtain biologically active proteins. Downstream processing thereby often includes the cell disruption step and the purification. Furthermore, overexpression of recombinant genes often results in formation of inactive protein aggregates, i. e. inclusion bodies, so that complicated and costly denaturation-refolding processes are necessary. Hence, extracellular protein production is highly desirable.

There have been developed a multiple approaches to enhance the extracellular yield and the secretion efficiency of recombinant proteins. One of the approaches, applied and investigated in this thesis, is usage of *leaky* mutants. Due to mutations in genes encoding for proteins of cell membrane and outer membrane proteins, these mutants show increased protein release from periplasm to extracellular milieu after the protein has been translocated by using natural bacterial translocation system.

Both single and triple knock out mutants, *ΔfhuA* and *ΔompAompCΔfhuA*, transformed with pAppA plasmid, have been cultivated and characterized according to their growth, protein production and enzyme activity with *E. coli* phytase AppA as reporter protein. Both strains were cultivated in 5 L bioreactors where the aim was to cultivate high cell density batch cultures.

2. THEORETICAL BACKGROUND

2.1. Composition of cell wall of *Escherichia coli*

The cell envelope of Gram-negative bacteria, such as *E. coli*, is composed of two lipid membranes enclosing an aqueous compartment called the periplasm. The cytoplasmic membrane is a symmetric phospholipid bilayer containing integral α-helical membrane proteins which forms the barrier between the cytoplasm and the periplasm and it is composed of approximately 70% phosphatidylethanolamine, 25% phosphatidylglycerol and 5% or less cardiolipin (McMorran *et al.*, 2014). The cytoplasmic membrane is a barrier for ions and enables a unique ionic composition of cytosol and energy-consuming processes that are triggered by the ionic gradients at the membrane. Furthermore, it prevents the uncontrolled traverse of proteins and other macromolecules that are synthesized in the cytosol but that fulfill their metabolic or structural functions on the outside of the cell. In order to allow passage of secretory proteins across the cytoplasmic membrane without compromising its structure and function, various transport mechanisms have evolved (Natale *et al.*, 2008). The periplasm is the compartment between the cytoplasmic membrane and the outer membrane, which contains soluble proteins (McMorran *et al.*, 2014), enzymes that catalyze the formation of disulphide bonds (Nakamoto and Bardwell, 2004; Ruiz *et al.*, 2006), as well as peptidoglycan cell wall (McMorran *et al.*, 2014). Periplasmic proteins play role in maintaining the integrity of the cell envelope. The primary energy source in the periplasm is proton-motive force across the inner membrane which is used by complex coupling mechanisms. Since no ATP is present in the periplasm, the processes which take place in this compartment are independent of nucleotide hydrolysis (McMorran *et al.*, 2014). The periplasm is an oxidizing environment (Nakamoto and Bardwell, 2004; Ruiz *et al.*, 2006) and it comprises around 10% of the total cell volume (McMorran *et al.*, 2014). The peptidoglycan layer is composed of glycan chains that are crosslinked by oligopeptides, but there are also proteins associated with the peptidoglycan layer such as Lpp (Braun's lipoprotein) that covalently anchors the peptidoglycan layer to the outermembrane (Ruiz *et al.*, 2006). The peptidoglycan cell wall plays important roles such as preventing lysis and maintaining the shape of the cell (McMorran *et al.*, 2014). The outer membrane is an asymmetric bilayer of lipopolysaccharide and phospholipid and contains β-barrel integral membrane proteins. The inner leaflet of the asymmetric outer membrane is comprised of

phospholipids. It is similar in composition to the cytoplasmic membrane, although the phosphatidylethanolamin content is enriched compared with the cytoplasmic membrane. The outer leaflet of the outer membrane consist of lipopolysaccharide (LPS), a glycolipid typically consisting of a core oligosaccharide, lipid A and an O-antigen. Low permeability of the outer membrane is due to the high number of fatty acid chains on lipopolysaccharide in contrast to phospholipids, and the fact that these chains are saturated. Both the inner and the outer membranes have associated lipoproteins on their periplasmic faces (McMorran *et al.*, 2014). Due to the high expression levels of pore-forming proteins and transporters that enable the diffusion of nutrients into the periplasm, the outer membrane is considerably more permeable than the cytoplasmic membrane (Faraldo-Gómez *et al.*, 2003).

2.2. Recombinant proteins

Proteins are the building blocks of life and all living forms synthesize them as part of their metabolism. They play a role in the cell cycle, cell signaling, cell adhesion and immune responses, and they form cytoskeleton. Special sort of proteins are enzymes which serve as biocatalysts, thus increasing the rate of metabolic reactions. Native and recombinant proteins are being used in the enzyme industry, the agricultural industry and the biopharmaceutical industry. The production of recombinant proteins requires the desired DNA getting cloned; then the protein is amplified in the chosen expression system. The use of recombinant DNA enabled that important genes, especially mammalian genes, could be amplified and cloned in foreign organisms. The cell cultures of bacteria, yeast, molds, plants, insects or mammals are being used as protein expression systems, so as transgenic plants and animals. The choice of the expression system for recombinant protein production depends on protein functionality, quality, yield and production speed. 39% of recombinant proteins are made by *E. coli*, 35% by CHO cells, 15% by yeasts, 10% by other mammalian systems and 1% by other bacteria and other systems. Generally, proteins smaller than 30 kD are expressed in a prokaryotic system while those larger than 100 kD are expressed in a eukaryotic system. One of the most commonly used hosts for the production of the heterologus proteins is enterobacterium *E. coli*. The advantages for choosing *E. coli* as the expression system are rapid growth, rapid expression, ease of culture and genome modifications, high product yields and the least expensive production. In addition, *E. coli* genetics are far better understood than those of any

other microorganism. The *E. coli* system has some drawbacks. *E. coli* is not suitable for production of proteins that require glycosylation and for S-S rich proteins as it cannot remove the S-S sequence. During high cell densities cultivation, the acetate is formed resulting in cell toxicity. This can be avoided by controlling the level of oxygen, by feeding glucose exponentially and keeping the specific growth rate below that which brings on acetate production. The proteins with many disulfide bonds are difficult to express and refolding of these proteins is difficult. Proteins which are produced as inclusion bodies are inactive, aggregated, insoluble and require refolding. In addition, some of the proteins are produced together with endotoxins. *E. coli* in not able to express very large proteins. In cases where glycosylation is necessary for proper folding or stability, recombinant yeast, mold, insect or mammalian cells are systems of choice (Demain and Vaishnav, 2009).

2.2.1. Recombinant protein production in *E. coli*

Recombinant proteins are generally produced either in microbial systems or in mammalian cell cultures. Advantages of microbial systems over mammalian cell cultures are production of recombinant proteins in a shorter time and at lower cost. Hence, bacteria are particularly suitable for producing recombinant proteins (Dassler *et al*., 2008). *Escherichia coli* has been the most commonly used host for mass-production of recombinant proteins of pharmaceutical and industrial importance. This production host has numerous desirable characteristics as easy manipulation, fast cell growth, high cell density cultivation and capacity to hold over 50% of foreign protein in total protein expression (Choi *et.al.,* 2006; Yoon *et al.,* 2010). However, *E. coli* cannot produce mammalian proteins that require post-translational modification for activity, or some proteins containing complex disulfide bonds (Choi and Lee, 2004). The usage of *E. coli* as cell factory for secretory production of recombinant proteins faces a few challenges for industrial production. Secretory production into the periplasm is physically limited by periplasmic volume and results in reduced cell growth and increased cellular burden. There is possibility that foreign proteins are degraded by host proteases. Also, target protein production is limited by insufficient capacity of the transport machinery. High rate of target translation can lead to accumulation inside the cell which results in inclusion body formation (Yoon *et al.,* 2010). Process that are particularly preferred for producing recombinant proteins in *E. coli* are those in which the target protein is secreted in the correct folding and in high yield directly into the fermentation medium (Dassler *et al*., 2008). Recombinant proteins can normally be produced in *E. coli* in various ways, i.e.

intracellular production as soluble protein, intracellular production as inclusion bodies, and secretion into the periplasm. In addition, it is possible to use leaky strains which have a defect in the outer membrane thereby releasing periplasmic proteins partly into the fermentation medium by a nonspecific mechanism. Examples of such leaky mutants are strains with altered lipoprotein contents in the outer membrane, e.g. lpp mutants which release the cell's periplasmic proteins into the fermentation medium. Such strains are extremely sensitive to various detergents, dyes and EDTA (Dassler *et al*., 2008). When the target exogenous proteins are expressed intracellularly in recombinant *E. coli*, cell disruption is necessary which often results in decrease of protein activities, the increase of sample impurities and pyrogen level (mainly from the cell membrane composition). In addition, intracellular accumulation of target proteins often results in the formation of inclusion body (Chen *et al.,* 2014). In comparison with cytosolic production, secretory production of recombinant proteins provides several advantages. Those advantages include simpler purification of recombinant proteins due to fewer contaminating proteins in the periplasm. Also, periplasmic space provides a more oxidative environment than the cytoplasm so that correct formation of disulfide bonds is facilitated. In addition, there appears to be much less protease activity in the periplasmic space than in the cytoplasm. Another advantage is that the N-terminal amino acid residue of the secreted product can be identical to the natural gene product after signal sequence is cleaved by a specific signal peptidase (Makrides, 1996; Choi and Lee, 2004). In order to obtain recombinant protein extracellularly secreted with *E. coli* cells, protein translocation is necessary across the two membranes – the cell membrane and the outer membrane. The advantages of extracellular secretion of target proteins are higher recombinant protein yield because the target protein accumulation is not limited by intracellular or periplasmic space, reduced risk of intracellular enzyme degradation, better environment for protein folding, and elimination of cell disruption step. Periplasmic expression of recombinant proteins can often be achieved with the help of a signal peptide. On the other hand, the available methods to overcome the outer membrane barrier for extracellular production of recombinant proteins are limited. In pursuance of solving this problem, various genetic attempts have been made to facilitate the extracellular secretion of recombinant proteins in *E. coli*, including optimization of codon and signal sequence, manipulation of transport pathways, fusion expression of outer membrane protein F, YebF or osmotically inducible protein Y and fusion expression of carrier protein which can be normally secreted extracellularly. Furthermore, the use of wall-less strains and the

coexpression of lysis-promoting proteins such as bacteriocin release protein (BRP) or colicin E1 lysis protein (Kil) have also been reported (Chen *et al.,* 2014).

2.3. Type II secretion mechanism

The type II secretion system is a two-step process for the extracellular secretion of proteins which includes periplasmic translocation and extracellular transport (Yoon *et al.,* 2010). In the the general secretory pathway (type II), proteins to be secreted contain an amino-terminal signal sequence that target them to the cytoplasmic membrane. During the translocation, signal peptidase removes the signal sequences. In the periplasm, proteins undergo transformations such as folding and assembly prior to translocation through the outer membrane (Pugsley, 1993; Sandkvist and Bagdasarian, 1996). Periplasmic translocation or secretion across the bacterial cytoplasmic membrane can be mediated by three pathways: the SecB-dependent pathway, the twin-arginine translocation (TAT) and the signal recognition particle (SRP) pathways (Mergulhão *et al.,* 2005). Concerted action of 12-16 proteins are constituting a secretion machinery named "secreton" which carries out a extracellular release of the periplasmic protein (Yoon *et al.,* 2010).

2.3.1. Sec translocation

Secretory proteins can be targeted to the Sec translocation complex by two different mechanisms, i. e., the co-translational and the posttranslational targeting. In the latter, the signal sequence containing secretory protein is released from the ribosome in its synthesis completed state and directed to the Sec-translocase. Posttranslational secretory proteins in various Gram-negative bacteria are guided to the Sec-translocase by the secretion specific chaperone SecB that maintains these proteins in a translocation-competent, unfolded state. During co-translational targeting, the signal recognition particle (SRP) binds to the signal sequence of the secretory protein while it emerges from the ribosome and the entire ternary complex of ribosome/SRP/nascent secretory protein chain are transferred from SRP to Sec-translocase. The signal peptide (signal sequence) is an amino-terminal extension of the secretory protein that is necessary for a correct targeting to the translocation pathway. The signal sequence typically has an average length of 20 amino acid residues with a tripartite structure, i.e., a positively charged amino-terminal (n-region), a hydrophobic core (h-region) and a polar carboxyl-terminal (c-region). The polar c-region is needed for recognition by the

type I signal peptidase (or leader peptidase), a membrane bound enzyme that cleaves the signal sequence from the mature secretory protein domain during or shortly after translocation. The tripartite structure of Sec signal sequences is recognized by the Sec components. The positively charged n-region has been implicated in electrostatic interactions with membrane phospholipids, whereas the hydrophobic core (h-region) typically consists of hydrophobic amino acids with a high propensity to form an α-helix. Both the n- and h-regions are critical structural elements recognized by the motor protein SecA and SRP. The binding affinity of SecA for signal sequences increases with the number of positive charges in the n-region, whereas the SRP interaction increases with the hydrophobicity of the h-region (Natale *et al.*, 2008).

2.3.1.1. SecB-dependent pathway

The vast majority of the secretory proteins of *E. coli* reach SecYEG post-translationally, after more than two-thirds of the chain has been synthesized at the ribosome. Here SecA is the SecYEG partner and the energizer of the system (Chatzi *et al.*, 2014). The bacterial Sec translocase is composed of a peripheral associated ATPase, SecA, and a membrane embedded protein conducting channel (PCC) that consist of three integral membrane proteins, SecY, SecE and SecG. The protein conducting channel forms a hydrophilic pore for secretory proteins to pass the membrane. The essential components of the Sec-translocase are the motor SecA and the channel subunits SecY and SecE. SecA can associate with low affinity with negatively charged phospholipids and binds with high-affinity to the PCC. Binding of SecA to SecYEG leads to conformational change of SecA (Natale *et al.*, 2008). SecY is an essential transmembrane protein which forms the central export pore and is stabilized and embraced by SecE (Chatzi *et al.*, 2014).   SecG is located at the periphery of the channel complex and it makes only limited contact with SecY and SecE (Natale *et al.*, 2008). While SecG may not be essential for viability or translocation, it facilitates the binding of SecA on SecY and its subsequent membrane insertion. Ten trans-membrane helices of SecY create a clamshell with its opening, known as lateral gate, facing the lipid bilayer thus allowing the hydrophobic signal sequences and trans-membrane helices to diffuse into the lipid bilayer (Chatzi *et al.*, 2014). The role of the n-region of signal peptide is believed to be targeting the preprotein to the translocase and binding to the negatively charged surface of the membrane lipid bilayer. It has been shown that increasing the positive charge in this region enhances translocation rates, presumably by increasing the interaction of the preprotein with

SecA. Furthermore, a minimum hydrophobicity of signal peptide is necessary for function and that translocation efficiency increases with the length and hydrophobicity of the h-region. On the SecB-dependent pathway, the ribosome-associated nascent chains of secreted proteins bind trigger factor, which is bound to the ribosomes. This association prevents cotranslational binding of the nascent chain to SRP components (Mergulhão *et al*., 2005). Soluble SecA appears as a functionally idle state and exhibits a low ATPase activity. Upon binding to SecYEG, the protein SecA attains its active state which manifests in conformational change of SecA and an increased rate of nucleotide exchange at SecA. SecB does not interact with the signal peptide region of secretory proteins, but binds to the polypeptide domains of long nascent secretory proteins while they emerge from the ribosome exit tunnel and stabilizes them in an unfolded conformation. Chaperone SecB is not essential for translocation. SecB facilitates translocation by maintaining secretory proteins in an unfolded conformation and actively targets and transfer secretory proteins to the PCC-bound SecA. In the absence of SecB, the signal sequence suffices to direct secretory proteins to the SecA. Unlike other chaperones, SecB binds specifically to the PCC-associated SecA, and this reaction initiates the transfer of the unfolded secretory protein from SecB to SecA (Natale *et al*., 2008). By bidning SecB to SecA, SecB releases the precursor protein that is transferred to SecA. SecA recognizes specifically the signal peptide of the preprotein. At this point SecA is bound to the SecY subunit of the SecYEG translocation complex. Binding of ATP at one of the two ATP-binding sites on SecA results in the release of SecB from the membrane. Binding of the preprotein to SecA causes translocation of approximately 20 amino acids. With subsequent binding of ATP to SecA, promoted is SecA membrane insertion and translocation of an additional 15-20 amino acids (Mergulhão *et al*., 2005), thus a loop of the signal sequence with the mature N-terminal region of the secretory protein inserts into the PCC (protein conducting channel). Here signal sequence gains access to the catalytic site of leader peptidase and processing may take place (Natale *et al*., 2008). The cleavage of the signal sequence occurs on the periplasmic face of the membrane (Chatzi *et al*., 2014). In a following step, SecA-bound ATP is hydrolysed and this results in release of the secretory protein from SecA while the inserted and translocated polypeptide domains remain trapped in the PCC (Natale *et al*., 2008). During every catalytic cycle of ATP hydrolysis, 20-30 amino acyl residues of the preprotein are translocated (Vassylyev *et al*., 2006; Chatzi *et al*., 2014). Next, the PCC-bound SecA may re-bind the protein without dissociating from PCC or SecA may dissociate from the PCC to allow a new SecA molecule to bind the translocation intermediate (Natale *et al*., 2008). Multiple rounds of SecA insertion and deinsertion from the membrane

promote protein translocation through the channel (Mergulhão *et al*., 2005), as well as hydrolysis of ATP (Natale *et al*., 2008), whereas proton-motive force (PMF) can complete translocation when the preprotein is halfway through the translocase. Despite being the most commonly used for recombinant protein production, the SecB-dependent pathway has one serious drawback. This system is not able to transport folded proteins and hence the secretion of proteins that fold rapidly in the cytoplasm may not be possible (Mergulhão *et al*., 2005).

2.3.1.2. SRP pathway

The signal recognition particle (SRP) pathway consists of several proteins and one RNA molecule (Mergulhão *et al*., 2005). SRP has a very high affinity for very hydrophobic signal sequences and nascent hydrophobic trans-membrane segments (Chatzi *et al*., 2014). By engineering the hydrophobicity of the signal sequence, recombinant proteins can be targeted to the SRP pathway (Mergulhão *et al*., 2005). During "co-translational" secretion, the Signal Recognition Particle (SRP), composed of the short 4.5S RNA species and the Ffh (Fifty four homologue) protein, recognizes and binds to the ribosomal L23 subunit (Chatzi *et al*., 2014), the site that overlaps the binding site of trigger factor (Mergulhão *et al*., 2005), and to the exiting signal sequence (Chatzi *et al*., 2014). Whether the peptide is targeted to the membrane via the SRP pathway, or post-translationally by the SecB pathway, is determined by the characteristics of the nascent peptide. The presence of an N-terminal signal sequence with a highly hydrophobic core, combined with a lack of a trigger factor binding site, results in cotranslational binding of the nascent chain to cytoplasmic protein Ffh. 4.5S RNA is required for binding of the nascent chain to Ffh (Mergulhão *et al*., 2005). Then ribosome-nascent chain complex is delivered to FtsY, its membrane-associated receptor (Chatzi *et al*., 2014), protein found both in the cytoplasm and at the membrane, thus releasing the nascent chain to the translocation site, presumably the SecYEG translocon (Mergulhão *et al*., 2005). The SRP-FtsY complex dissociates at the expense of GTP (Chatzi *et al*., 2014).

2.3.2. TAT pathway

The Tat pathway appears to be the unique in its ability to transport relatively massive folded proteins across energy-transducing cytoplasmic membrane (Robinson et al., 2011). The twin-arginine translocation system does not require ATP as an energy source, and relies solely on the proton motive force (PMF) (Patel et al., 2014). The Tat system's best-known substrates are redox proteins that bind their cofactors in the cytoplams, such as FeS, NiFe centres and molybdopetrin, prior to export to the periplasm (Robinson et al., 2011). However, there are also Tat substrates which lack cofactors. Obviously, cofactor assembly is not the only reason for Tat dependent transport (Natale et al., 2008). The substrates for the Tat pathway are exported posttranslationally in a process mediated by N-terminal signal peptides. Many Tat substrates are cofactor-containing, so that after synthesis and initial folding they acquire redox cofactors in the cytoplasm, often with the aid of chaperones and substrate-specific guidance factors (Robinson et al., 2011). Furthermore, there are many general and specific chaperones which can bind Tat signal sequences and help to protect Tat signal sequences degradation. The term "proofreading" is used to describe a function that prevent targeting prior to folding, which includes specific chaperones that prevent translocase interactions prior to cofactor insertion and folding, leading in many cases to an oligomerization of the substrate protein (Natale et al., 2008). The TAT system is capable of secreting folded proteins by employing a particular signal peptide containing a twin-arginine sequence (Choi and Lee, 2004). TAT signal peptides are composed of three regions as well as Sec signal peptides: a c-region that contains the cleavage site, a hydrophobic region (h-region) and a positively charged region (n-region) (Mergulhão et al., 2005). Studies on Tat signal peptides revealed a highly conserved SRRxFLK motif (where x is a polar amino acid (Robinson et al., 2001)), where three determinants appear to be important: the twin-arginine pair, the hydrophilic -1 residue and the hydrophobic +2 residue (-/+ relative to the twin-arginine pair). The C-region of certain Tat signal peptides houses basic residues, which are seldom found in the same region of Sec signal peptides. The C-terminal region contains an A-x-A motif, which is a consensus cleavage site for removal of the signal peptide by signal peptidase. The Tat signal peptides are longer than Sec-specific signals (on average 38 to 24 amino acids, respectively) (Patel et al., 2014) and usually, the hydrophobic region of TAT signal peptides is less hydrophobic in comparison with that of Sec leader peptides (Mergulhão et al., 2005). On the TAT pathway, the substrate bearing a twin-arginine signal peptide binds initially to TatBC

complex in a resting membrane. Bounding of the precursor to the substrate-binding TatBC complex, results in the association of the TatA complex with the TatBC complex in the presence of a ΔpH (Patel e*t al*., 2014). The substrate is then transported by a mechanism requiring the proton motive force, after which it is processed to the mature size (Robinson e*t al*., 2011). Once the transport has been done, TatA disassembles from TatBC and the Tat substrate is released from the membrane by a cleavage of type I signal sequences peptidases (Yahr and Wickner, 2001; Natale *et al*., 2008). Three integral membrane proteins, TatA (9.6 kDa), TatB (18.5 kDa) and TatC (28.9 kDa), usually constitute the Tat translocase system. These proteins are encoded by the *tatABC* operon and reside in the cytoplasmic membrane arranged as a Tat(A)BC substrate binding complex and a separate TatA complex. In *E. coli*, there is no evidence for a specific role of TatE, a paralog of TatA, and it is encoded elsewhere in the genome. Both TatA and TatB are single-span transmembrane proteins that possess a highly charged, unstructured cytoplasmically-exposed C-terminus, single-span transmembrane helix; hinge region; amphipathic helix lying along the cytoplasm-membrane interface and a short periplasmic N-terminal region. In contrast, TatC is a polytopic protein that presumably contains 6 transmembrane spans, with both the N- and C- termini in the cytoplasm. The *tatABC* gene products form two distinct membrane complexes at steady state: a separate TatA complex and a TatBC-containing substrate binding complex where most of TatB and –C are found at 1:1 stoichiometric ratio. TatC is the largest and most conserved component of the Tat pathway where it plays a central role in the translocation event, ranging from substrate recognition and binding, to the recruitment of other Tat components (Patel e*t al*., 2014). Although TatA and TatB share 25% sequence identity and the two subunits have a similar secondary structure, these two subunits cannot substitute for each other, even when they are overexpressed (Sargent *et* al., 1999; Robinson e*t al*., 2011). It is believed that physiological role of Tat system is to extend the set of translocatable substrates to those that fold prior to translocation and that it is used only in cases where cytoplasmic folding excludes the use of the Sec system (Natale *et al*., 2008). It has been reported that transport via the TAT pathway is slower and less efficient than the Sec pathway. Furthermore, it has been shown that this secretion mechanism is rapidly saturated, so that coexpression of the *tatABC* operon is required for large-scale production. The requirement for coexpression presents a severe disadvantage for the application of the TAT pathway for production processes. However, unlike the SecB or the SRP pathways, the TAT pathway is capable of transporting folded protein across the inner membrane (Mergulhão *et al*., 2005), especially proteins that contain

complex disulfide bonds or that may be folded before they reach the Sec machinery (Choi and Lee, 2004).

2.4. Leaky mutants

Leaky mutants of *E. coli* are mutants which, owing to mutations in structural elements of the outer cell membrane or the cell wall, show increased release of periplasmic proteins into the medium (Shokri *et al*., 2003; Wich and Dassler, 2008) and allow the entry of molecules (Ruiz *et al*., 2006). Weakened cell wall contributes to the cell sensitivity due to influences from the outer environment (Wang, 2002). A set of precisely defined, single-gene deletions of all nonessential genes in *Escherichia coli* K-12 strain BW25113 was made to create the KEIO strain collection. *Escherichia coli* K-12 has been one of the best-characterized organisms in molecular biology. BW25113 is a strain with a well-defined pedigree that has not been subjected to mutagens. Open-reading frame coding regions were replaced with a kanamycin cassette flanked by FLP (flippase) recognition target (FRT) sites by using a one-step method (λ Red system) for inactivation of chromosomal genes and primers designed to create in-frame deletions upon excision of the resistance cassette. Of 4186 genes targeted, mutants were obtained for 3864. Two independent mutants were saved for every deleted gene in order to alleviate problems encountered in high-throughput studies (Baba *et al*., 2006). *E. coli* JW0146-2 strain has *fhuA* deleted which codes for a monomeric protein FhuA, a β barrel composed of 22 antiparallel transmembrane β strands (Ferguson *et al*., 1998). FhuA protein (*f*erric *h*ydroxamate *u*ptake protein component *A*, 714 residues) has a physiological function in the uptake of the siderophore ferrichrome, i.e., it facilitates ligand-gated transport of ferrichrome-bound iron across outer membranes (Locher *et al*., 1998). In addition to bining ferrichrome-iron, FhuA in the outer membrane of *Escherichia coli* also functions as the primary receptor for the structurally related antibiotic albomycin, for the bacterial toxin colicin M, for the peptide antibiotic microcin 25, and for several bacteriophages (T1, T5, UC-1, and φ80) (Ferguson *et al*., 1998). Another strain used in this thesis is triple knock-out strain Δ*ompA* Δ*ompC* Δ*fhuA*. Gene *ompA* codes for OmpA - outer membrane protein A, the most well-studied major outer membrane protein in *E. coli* (Wang, 2002) with typically 100 000 copies per cell (Ortiz-Suarez *et al*., 2016). The outer membrane protein A (OmpA) which

forms a non-specific diffusion pore is a 325-residue protein and it is the most common protein component of the outer membrane of *E. coli* (Ishida *et al*., 2014). The function of heat-modifiable OmpA is thought to contribute to the structural integrity of the outer membrane, along with peptidoglycan-associated lipoprotein and murein lipoprotein, by holding peptidoglycan and the outer membrane together as the whole structure in *E. coli*. Furthermore, OmpA serves as a receptor of colicin and several phages, it is required for F-conjugation and some small molecules may pass the β-barrel of OmpA and cross the outer membrane (Wang, 2002). Within the outer membrane resides the N-terminal domain of OmpA which is an eight-stranded transmembrane β-barrel. The soluble C-terminal domain is located in the periplasm. A 15-amino-acid linker region connects the barrel to the C-terminal domain (Ortiz-Suarez *et al*., 2016). The β-barrel of OmpA can be in either an open or closed state, thus causing different levels of conductance (Ortiz-Suarez *et al*., 2016). Wang has propored that OmpA is composed of three functional domains including a hydrophilic extracellular mass, a β-barrel transmembrane structure, and a peptidoglycan binding domain (Wang, 2002). Second gene, *ompC* codes for protein OmpC. It belongs to a group of porin proteins which form relatively nonspecific pores which allow diffusion of nutrients across the outer membrane, facilitate the transport of colicins and serve as receptors for various bacteriophages. It is tightly associated with peptidoglycan and lipopolysaccharide (Misra and Benson, 1988). The sequence of OmpC is 60% identical to another porin, OmpF. OmpC is slightly more cation selective than OmpF and its pore has been predicted to be smaller (Nikaido, 2003; Baslé *et al.*, 2006). Both major outer membrane proteins OmpC and OmpF in *E. coli* are known as porins because they form passive diffusion pores which allow small molecular weight hydrophilic materials across the outer membrane (Nikaido, 1979; Mizuno *et al*., 1983). In *E. coli* they are among the most abundant outer membrane proteins with about 10^5 copies per cell and serve as general pathways for the influx of small molecules (e.g. molecular weight under 600) (Masi and Pagès, 2013). Many environmental factors have been identified that alter OmpF and OmpC expression, including temperature, pH, osmolarity, nutrient availability, and various toxins (Forst and Inouye, 1988; Pratt *et al*., 1996; Liu and Ferenci, 2001; Batchelor *et al*., 2005).

2.5. Phytase AppA

Phytates are the primary storage form of both phosphate and inositol in plants, predominantly occurring in cereal grains, oilseeds and legumes (Haefner *et al.,* 2005). Phytase (myo-inositol

hexakisphosphate phosphohydrolase, EC 3.1.3.8 for 3-phytase and 3.1.8.26 for 6-phytase) catalyses the release of inorganic phosphate and myo-inositol from phytate (myo-inositol hexakiphosphate) (Pandey *et al.,* 2001), the salt of phytic acid (Haefner *et al.,* 2005). Phytic acid (myo-inositol 1,2,3,4,5,6-hexakis dihydrogen phosphate) is a polyanionic chelating agent that forms insoluble complexes with nutritionally important cations, e.g., Ca^{2+}, Fe^{2+}, Mg^{2+}, Zn^{2+},Cu^{2+} and Mn^{2+} (Haefner *et al.,* 2005), thereby decreasing their bioavailability (Greiner et al., 1993). Furthermore, it can also form complexes with amino acids and proteins at both alkaline and acidic pH. Microbial phytase is able to enhance protein digestibility (Haefner *et al.,* 2005). Phytase has been added as a supplement to animal feed for monogastric animals to eliminate the negative effects of phytic acid in animal nutrition and to enhance plant phosphorous utilization (Morz *et al.,* 1994, Miksch e*t al.,* 2002). Phytase is used in commercial diets of swine, poultry and fish to improve the availability of energy, phosphorous, minerals and amino acids. Without enzymatic degradation by phytases, the phytate molecule together with nutrients bound to it, cannot be absorbed in the digestive tract and consequently accumulates in fecial material. Since the availability of phosphorous in plant-derived animal food is low, diets for nonruminants have been supplemented with inorganic phosphates. The manure of livestock has been applied to the soil, thus leading to accumulation of phosphate in the soil. Outcome of this could be long-term leaching of phosphate into ground water and eutrophication of surface waters. Phosphorus excretion of monogastric animals can be reduced between 25 and 50% by replacing inorganic phosphates with microbial phytase (Haefner *et al.,* 2005). Phytase activity in microorganisms occurs most frequently in fungi, in particular *Aspergilli*, bacteria, yeast and rumen microorganisms (Greiner e*t al.,* 1993). Main features of *E. coli* phytase are the highest specific activity of all phytases tested so far and in contrast with commonly used *Aspergillus* phytases, the pH optimum is situated more in the acid range and *E. coli* phytase is resistant to proteolytic degradation in stomach of monogastric animals (Miksch e*t al.,* 2002). Furthermore, *E. coli* phytase is more resistant to high temperatures during pelleting process (Kleist *et al.,* 2003). *E. coli* phytase is a periplasmatic 6-phytase (Greiner *et al.*, 1993) with a molecular weight of about 45000 (with signal sequence being cleaved) and an isoelectric point of 6.3 (Dassa *et al.*, 1980). Since the phytase is periplasmic enzyme, extracellular production is required for this industial enzyme in order to facilitate downstream processing, e.g. cell disruption and the separation of cell debris (Miksch e*t al.,* 2002).

2.6. Bioreactor cultivation of *Escherichia coli*

The overall goal in production of recombinant proteins is to simultaneously reach a high cell density, a high product quality and a high specific recombinant protein production rate. A high cell density can only be achieved by fed-batch cultivation that corresponds to a feed profile, which leads to a continuously decreasing growth rate during the process (Shokri *et al.,* 2003). However, the extended culture period in fed-batch cultures is the reason why the production of acetate is greater in fed-batch rather than in batch culture (Lee, 1996). High productivities are obtained through either a high concentration or a high activity of the bio-catalyst (Knoll *et al*., 2007). Cultivation of *E. coli* to high cell concentrations is necessary for obtaining the maximal volumetric productivities. In response to excess carbon or oxygen limitation, cells produce growth-inhibiting acidic by-products of incomplete substrate oxidation such as acetic acid. Prevention of the accumulation of toxic levels of acetic acid is the main task for achieving high cell concentrations in bioreactors (Korz *et al.,* 1995). Development of high cell density culture (HCDC) techniques for cultivation of *E. coli* cells has improved productivity and provided advantages such as lower production costs, reduced investment in equipment, reduced wastewater, enhanced downstream processing and reduced culture volume (Lee, 1996). Some of the problems that can arise in high-cell-density cultures are limited capacity for O_2 supply, limitation and/or inhibition of substrates and formation of metabolic by-products. In addition, the final cell density can be limited by a several factors such as formation of metabolic by-products, heat and generation of CO_2 (Riesenberg, 1991). Temperature of cultivation impacts cell metabolism. Nutrient uptake and growth rate can be reduced by lowering the culture temperature from 37°C to 26-30°C. This results in reduced formation of toxic by-products and the generation of metabolic heat. Furthermore, it also reduces cellular oxygen demand and formation of inclusion bodies. High partial-pressure of CO_2 (>0.3 atm) stimulates acetate formation and reduces growth rate. With the increase of bioreactor size, efficiency of mixing is being reduced causing unequal distribution of nutrients in HCDCs. It has been demonstrated that some nutrients, such as nitrogen and carbon sources, can inhibit cell growth when they are present above a certain concentrations. For example, glucose inhibits growth at concentration above 50 g L^{-1}, ammonia at concentration above 3 g L^{-1} and phosphorus at concentration above 10 g L^{-1}. Therefore, HCDCs are started with concentrations of nutrients below the inhibitory thresholds and as necessary to maintain high growth rates. Three types of media have been known: defined,

semi-defined and complex. It is necessary that medium for growing cells to a high density contains all the necessary components for supporting cell growth, while avoiding inhibition. In HCDCs ammonium hydroxide is often used both as a nitrogen source and as a base for adjustment of culture pH (Lee, 1996). The formation of metabolic by-products, such as acetate, ethanol, D-lactate and L-glutamic acid, during aerobic growth in media containing glucose, pyruvate, glycerol and/or complex components might become a serious problem if the by-products accumulate to concentrations which inhibit the growth (Riesenberg, 1991). The major problem in fermentation is the formation of acetate resulting in cell toxicity. Acetate is produced when *E. coli* is grown under anaerobic or oxygen-limited conditions. Also, it has been shown that *E. coli* cultures growing in the presence of excess glucose can also produce acetate even under aerobic conditions. A high concentration of acetate (i.e., above 5 g L^{-1} at pH 7) inhibits the growth rate and reduces biomass yield (Kleist *et al.* 2003). Production of acetate happens when carbon flux into the central metabolic pathway exceeds the capacity for energy generation within the cell and biosynthetic demands; the main cause can be saturation of the electron transport chain and/or the tricarboxyl acid (TCA) cycle. Under aerobic conditions, there are two enzymatic pathways for formation of the main by-product acetate. The major one is the acetate kinase phosphotransacetylase pathway starting from acetyl-coenzyme A, and in the minor one acetate is derived directly from pyruvate by pyruvate oxidase. Low solubility of oxygen is limiting factor in HCDCs. Oxygen limitation can be prevented by increasing the aeration rate or agitation speed, using oxygen-enriched air or pure oxygen (Lee, 1996), decreasing the temperature and pressurizing the culture (Riesenberg, 1991). Concentration of the saturated dissolved oxygen (DO) in water at 1atm and 25°C is about 7 mg L^{-1} (Lee, 1996). Hence, the challenging task in biochemical engineering presents sufficient oxygenation of aerobic fermentation process, especially in high cell density cultivation (HCDC) where the oxygen demand exceeds by far the maximum oxygen transfer capacity (OTR$_{max}$) of conventional bioreactors such as bubble columns or stirred tanks. The microbial growth and activity are limited by the dissolved oxygen concentration in the culture medium. Oxygen limitation results in diminish of the growth and production rates and for the microorganisms which are capable of anaerobic metabolism, the metabolic pathway can be shifted in an unfavorable direction thus declining product yield. The most commonly applied for overcoming oxygen limitation by increasing the OTR$_{max}$ of bioreactors are aeration using oxygen enriched air and special aeration systems (Knoll *et al.*, 2007).

3. MATERIALS AND METHODS

3.1. Chemicals

Following table (Table 1.) lists all used chemicals and their manufacturers. In Table 2., there is a list of special chemicals – kits and ladders (Figure 1.). Chemicals are dissolved in ddH_2O except for 4-Nitrophenyl phosphate disodium salt hexahydrate, which is dissolved in glycine-HCl buffer made as explained later in chapter *Enzyme activity test*.

***Table 1.** List of used chemicals and their manufacturers.*

Chemicals	manufacturer
4-Nitrophenol	Sigma-Aldrich Chemie GmbH
4-Nitrophenyl phosphate disodium salt hexahydrate	Sigma-Aldrich Chemie GmbH
agar – agar	Carl Roth GmbH + Co. KG
ammonium persulphate	Carl Roth GmbH + Co. KG
Bis-/Acrylamide (0,8 %, 30 %)	Carl Roth GmbH + Co. KG
bromophenol blue	Carl Roth GmbH + Co. KG
BSA (albumin fraction V)	Carl Roth GmbH + Co. KG
Coomassie Brilliant Blue G – 250	Carl Roth GmbH + Co. KG
dipotassium phosphate	VWR International GmbH
glycerine (99,5 %)	Emery Oleochemicals GmbH
Glycine	Carl Roth GmbH + Co. KG
IPTG	Carl Roth GmbH + Co. KG
Isopropanol	VWR International GmbH
kanamycin sulphate	Carl Roth GmbH + Co. KG
natrium carbonate	Carl Roth GmbH + Co. KG
natrium chloride	Fisher Scientific GmbH
natrium hydroxide	Carl Roth GmbH + Co. KG

phosphoric acid	Carl Roth GmbH + Co. KG
Pluronic (antifoam)	BASF SE
potassium dihydrogen phosphate	VWR International GmbH
SDS	Carl Roth GmbH + Co. KG
soya peptone	UD Chemie GmbH
TEMED	Carl Roth GmbH + Co. KG
Tris	Fisher Scientific GmbH
Tris-HCl	Fisher Scientific GmbH
yeast extract	Ohly GmbH
$CaCl_2$	PanReac AppliChem ITW

Table 2. *Special chemicals and their manufacturers.*

Chemical	manufacturer
PageRuler Prestained Ladder	Thermo Fisher Scientific Inc.
Roti®–Nanoquant kit for protein concentration test K880	Carl Roth GmbH + CO. KG
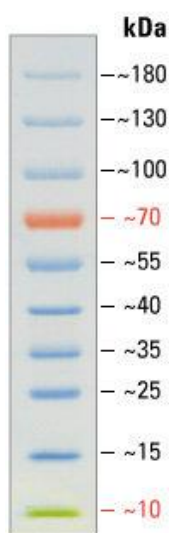
Figure 1. *PageRuler Prestained Ladder by Thermo Fisher Scientific Inc. on SDS electrophoresis gel. (www.thermofisher.comordercatalogproduct26616, access date May 4, 2018)*

3.2. Devices and lab consumables

Tables in this chapter show list of all used devices, their model and manufacturer, as well as lab consumables and their manufacturers.

Table 3. *List of used devices with respective model and manufacturer.*

Device	Model	manufacturer
autoclave	V – 150 D – 65	Systec GmbH
heat block	Blockthermostat BT 100	Kleinfeld Labortechnik GmbH
light microscope	BX40	Olympus Corporation
magnet mixer	IKAMAG REO	IKA
pH - meter	691	Metrohm AG
Shaker	Lab – Shaker LS – X	Kühner AG

spectrophotometer	BioPhotometer	Eppendorf AG
spectrophotometer (microplates)	SPECTRA MAX 250	Molecular Devices Corporation
Ribolyser	TeSeE PRECESS 24	Bio-Rad Laboratories
Vortex	Vortex – Genie 2	Scientific Industries, Inc.
Centrifuges	3-30KS 1-15	Sigma Laborzentrifugen GmbH
orbital rocking shaker	POLYMAX 2040	Heidolph Instruments GmbH and Co. KG
electrophoresis power supplier	Standard Power Pack P25	Biometra GmbH
analytical balance	PM34-K DeltaRange	Mettler – Toledo GmbH
agarose gel electrophoresis system	MINI GEL II	VWR International GmbH
precision balance	AE 260 DeltaRange	Mettler – Toledo GmbH
Freezer	MDF – U5386S	SANYO Electric CO., Ltd
vacuum dryer	VT 5042 EK	Heraeus
ultrasound homogenizer	Sonifier 450	BRANSON

Table 4. *List of used lab consumables and their manufacturers.*

Item	manufacturer
BRANDplates® (96–well microplates), polystyrene: 350 µL	Brand GmbH + Co. KG
cuvette, polystyrene, 1.5 mL	Brand GmbH + Co. KG

pipette tips, polypropylene: 1000, 200 and 10 µL	Greiner Bio-One AG
microcentrifuge tube, polypropylene: 1,5 mL and 2 mL	Greiner Bio-One AG
Erlenmeyer flask with baffles, glass: 300 ml, 500 mL and 1000 mL	Schott Duran
Erlenmeyer flask, glass: 300 mL	Schott Duran
conical centrifuge tubes, polypropylene: 15 mL and 50 mL	Greiner Bio-One AG

3.3. Software

Table 5. below shows list of software used in this thesis.

Table 5. List of used software and respective developer companies.

Name	developer company
SoftMax® Pro	Molecular Devices Corporation
BiOSCADA Lab	BIOENGINEERING

3.4. Growth media

In this thesis, two different media were used: LB medium (*Luria – Bertani*) to grow a preculture and make glycerine cultures, and TB medium (*Terrific broth*) to grow main culture in flasks as well for the cultivation of bacteria in the bioreactor (Table 5. and 6.). If needed, kanamycin was added to a final concentration of 50 µg/mL. Media were sterilized in autoclave in 121 ºC and pressure of 1 bar.

Table 6. Composition of Luria-Bertani medium, pH 7,4.

Component	concentration [g/L]

Component	concentration [g/L]
soya peptone	10
yeast extract	5
sodium chloride	10

*to make agar plates, 15 g/L agar-agar added

Table 7. *Composition of Terrific broth medium*

Component	concentration [g/L]
soya peptone	12,0
yeast extract	24,0
Glycerine	5,0
dipotassium phosphate, K_2HPO_4*	12,5
potassium dihydrogen phosphate, KH_2PO_4*	2,4

* autoclaved separately from other components

3.5. Plasmid

In this paper plasmid pAppA1 was used. Figure 2. below shows plasmid map which contains all important features closely explained in Table 8.

Figure 2. Map of plasmid pAppA1 made with SnapGene software, GSL Biotech LLC.

Table 8. Explanation of abbreviations on plasmid map showed on Figure 2. above.

Contractions	meaning
AppA	phytase AppA from *E. coli* with native signal sequence for translocation
BlaP	promoter for ampicillin resistance
KanR	kanamycin resistance
AmpR	ampicillin resistance
LacI	repressor for binding to lac-operator
ori	high copy origin of replication, ColE1/pMB1/pBR332/pUC
T5 promoter	promoter induced by IPTG

| rrnB1 B2 T1 txn terminator | structural terminator |
| M13 forward | the binding site for primer |

3.6. Bacterial strains

In Table 9. below, there is a list of *E. coli* strains used for this thesis. Each of them is transformed with previously explained plasmid pAppA1.

Table 9. List of bacterial strains with respective genotype used in Working Group Fermentation technology laboratory. Strains are originally from KEIO collection and deletions written in column "strain" were made in Laboratory for Fermentation Technology.

Strain	genotype
E. coli JW0146-2 CGSC 8416 KEIO Δ*fhuA766*	*F-, Δ(araD-araB)567, ΔfhuA766::kan, ΔlacZ4787(::rrnB-3), λ-, rph-1, Δ(rhaD-rhaB)568, hsdR514*
E. coli JW0940-6 Δ*ompA* Δ*ompC* Δ*fhuA*	*F-, Δ(araD-araB)567, ΔlacZ4787(::rrnB-3), λ-, ΔompA772 rph-1, Δ(rhaD-rhaB)568, hsdR514, ΔompC, ΔfhuA::kan*

3.7. Methods

3.6.1. Preculture setting

To grow preculture, 50 µL of glycerine culture was added to 30 mL of LB medium (composition described in chapter Growth media) and grown in 300 mL flasks without baffles. Preculture used for bioreactor cultivation is grown in 100 mL of LB medium in 1 L flasks with baffles. Also, kanamycin is added in final concentration of 50 µg/mL. Preculture was cultivated on shaker (120 rpm, 50 mm rotation radius) for 16 hours on 37º C.

3.6.2. Strain stock

To keep bacterial culture over longer time, 800 µL of preculture was added to 200 µL of 87 % glycerine in a 1,5-mL reaction vessel. Then, the sample was mixed on vortex and frozen in liquid nitrogen. Glycerine culture was kept in -80º C. Short time storage of samples to be analysed was in -20 ºC. Agar plates were stored in -4 ºC.

3.6.3. Flask cultivation

To set a main culture, in 1000 mL Erlenmeyer flask with four baffles, 100 mL of TB medium was added. Also, kanamycin was added in final concentration of 50 µg/mL. Volume of inoculum, i.e. preculture, was calculated to set the initial OD_{600} value to 0.2. Cultivation was performed on a shaker (120 rpm, 50 mm rotation radius) at 37 º C until OD_{600} reached a value between 0.8 and 0.9. At this point, IPTG as inductor was added to a final concentration of 1 mM. Samples from each of three biological replicates were taken at three time points: 0 hours (immediately after induction), 1 hours, 2 hours, 3 hours, 4 hours, 5 hours, 6 hours and 24 hours after induction. 500 µL- samples were taken in each time point for measuring OD_{600} and microscopy control.

To get supernatant samples, 500 µL from each biological replicate was taken and centrifuged for 10 minutes at 4 º C and 7000 g. Supernatant samples were stored at -20 º C.

Also, 1 mL of cell culture from each biological replicate was taken and stored at -20 º C for SDS-PAGE.

3.6.4. Bioreactor cultivation

Selected strains were cultivated in a bioreactor. TB medium was used as a nutrient medium (composition in chapter *Materials*) to which, after sterilization, antibiotic kanamycin was added to final concentration of 50 µg/mL. Additionally, inductor IPTG was added to final concentration of 1 mM when the OD_{600} was around 1. The software BiOSCADA Lab by BiOENGINEERING was used to follow the course of fermentation and collect process data.

The single knock-out *E. coli* strain *ΔfhuA* and the triple knock-out *ΔompAΔompCΔfhuA* were cultivated in bioreactor NLF 3. The total volume of the bioreactor was 7 L while the working volume was 5 L. Conditions of cultivation are shown in Table 10. below.

Table 10. *Conditions of cultivation in bioreactors.*

conditions	bioreactor NLF 3
pH	7.4
temperature	37° C
overpressure	0.2 bar
air flow	5 NL/m
pO$_2$	30 %
stirrer speed	92-1067 rpm

To keep a constant pH during fermentations, 10 % phosphoric acid and 2 M NaOH are used and sterilized prior to use as well as antifoam Pluronic.

A stirrer cascade is used to control oxygen concentration in nutrient medium. The lower limit was 92 rpm (*rotations per minute*) and the upper one 1067 rpm. pO2 signal is adjusting pO2 level and if the level is lower than the setpoint, the pO2 control-unit gives a signal to the stirrer control unit to increase the stirrer frequency.

Cell growth was monitored by measuring optical density. Initial cell density was 0.2. Samples were taken by autosampler. After induction, samples were taken at sixteen time points. First sample was taken right after the induction and others were taken every hour until sixth hour after induction. Afterwards, every two hours samples were taken until twenty-fourth hour after the induction. Samples were taken aseptically using a steam-sterilisable sampling valve of bioreactor and prepared in a same way as described in chapter *Flask cultivation.*

Bioreactor specification is attached in *Appendix*.

3.6.5. Cell lysis

Sonication is used to lyse bacterial cells cultivated in flasks in following way: 1 mL of defrosted sample was put in an ice-water bath and sonicated in three cycles for 30 seconds with 30 seconds break in between the cycles. Ultrasound homogeniser settings were: *Timer*

on *hold*, *Duty Cycle* on *constant* and *Output Control* was set on 2. The efficiency of sonication is monitored by microscopy. If cells were not disrupted, another cycle of sonication is repeated. Then, samples were centrifuged for 10 minutes on 4 ° C and 16000 g. The precipitate was discarded, and the supernatant was kept on -20 ° C.

Cells were lysed mechanically in a Ribolyser TeSeE PRECESS 24 Homogenizer cell disrupter at speed 6500 rpm, three times for 30 s. 800 µL of defrostet sample were taken. The efficiency of cell lysis is monitored by microscopy. If cells were not distupted, another cycle is repeated. Then, samples were centrifuged for 10 minutes on 2 ºC and 14 000 rpm. The precipitate was discarded, and the supernatant was kept on -20 ° C.

3.6.6. Making chemically competent cells

To set a main culture, in 300 mL Erlenmeyer flask, 60 mL of LB medium was added. Also, kanamycin was added in final concentration of 50 µg/mL. Volume of inoculums, i.e. preculture, was calculated to set the initial OD_{600} value to 0.2. Cultivation was performed on a shaker (120 rpm, 50 mm rotation radius) at 37 ° C until OD_{600} reached a value between 0.8 and 0.9. Then the cultivation stopped, and the cell culture was cooled down on ice for 15 min. The cell culture was then centrifuged for 10 min at 4 ° C and 4000 g. The supernatant was discarded. The residues of the supernatant were absorbed with paper. The cells were resuspended in 2 mL of ice cold buffer 1. Afterwards, the cells were centrifuged for 10 min at 4 ° C and 4000 g. The supernatant was discarded. The cells were resuspended in 2 mL of ice cold buffer 2. 100 µL of sample was poured in 1.5 mL vessel and frozen in liquid nitrogen. The samples were stored in -80 ° C.

3.6.7. Transformation of chemically competent cells

100 µL of sample was melted on ice. 1 µL of DNA was added and incubated on ice for 20 min. Then, it was incubated in 42 ° C water bath for 30 s and left on ice for 2 min. 500 µL of LB medium was added and incubated on a shaker for 1 h at 37 ° C. Afterwards, samples where centrifuged for 2 min and 7000 rpm at room temperature. 500 µL of the supernatant was discarded, and cells were resuspended with pipette in 100 µL of supernatant. The transformed cell suspension was then pipetted on LB agar plates containing kanamycin.

3.7.Analytical methods

3.7.1. Optical density measurement

During the cultivation, bacterial growth was monitored by measuring optical density (OD600). Using photometer (BioPhotometar by Eppendorf AG), absorbance is measured on wavelength of 600 nm. To stay in linear range (0 – 0.9), samples are diluted with respective medium in disposable polystyrene cuvette (1.5 mL, Brand GmbH & Co. KG) prior to measurement. Respective medium was used as a blank.

3.7.2. Microscopy

A few drops of cell suspension were diluted on a slide and observed under BX40 light microscope by Olympus Corporation with magnification 200x. Sample photos were taken and saved using IC Capture 2.0 software by Imaging Source Europe GmbH.

3.7.3. Enzyme activity test

Acid phosphatase activity test with *pNPP* (*para*-nitrophenylphosphate) is used to quantify the enzyme activity in both supernatant and total enzyme activity (in cell lysate and supernatant together). Samples and standards are diluted in fresh 0.25 M glycine–HCl buffer, pH 2.5. Supernatants are diluted in a range of 1:10 to 1:400 and disrupted cell samples in a range of 1:40 to 1:700.

Pipetting schedule in 96-well plate is shown on Figure 3. below.
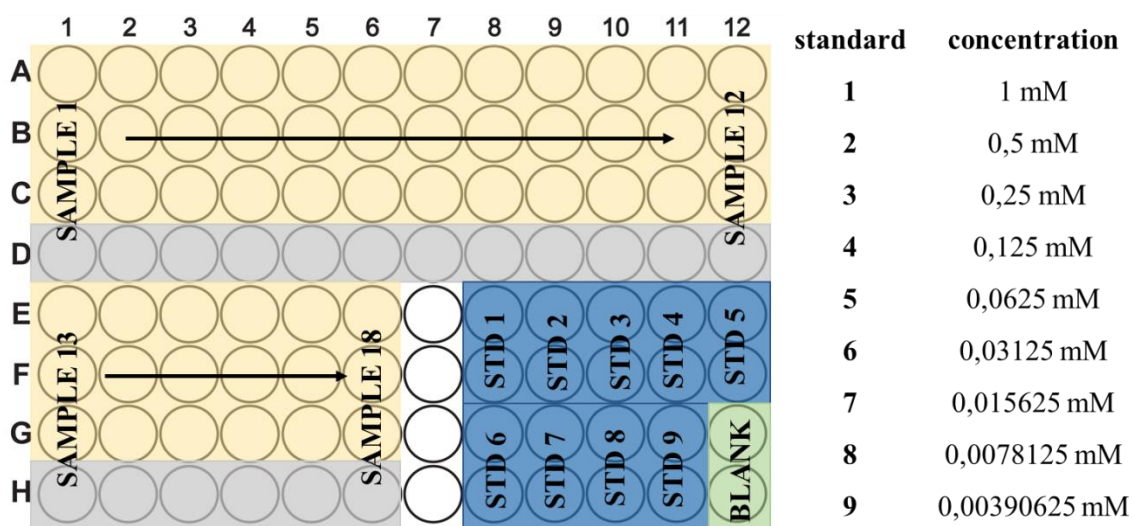
Figure 3. Pipetting schedule for enzyme activity test. Yellow colour stands for samples (pipetted in three replicates) in which substrate was added, grey colour stands for samples in which buffer was added instead of substrate, blue colour stands for standards and green colour for blank (buffer only), both pipetted in two replicates. On the right side, there are concentrations of standard para-nitrophenol.

50 µL of samples and standards was pipetted in a 96-well plate and incubated in a thermostat in 50 ºC for exact 15 minutes as well as the substrate solution, 50 mM *para*-nitrophenylphosphate (*pNPP*) dissolved in 0.25 M glycine–HCl buffer. After 15 minutes of incubation, 50 µL of substrate or buffer is added to samples and standards (see figure above). The reaction is stopped after 10 minutes by adding 100 µL of stop solution (1 M sodium carbonate) in each well, causing a change of colour from colourless to yellow. Thereafter, A_{405} was measured using software SoftMax® Pro. Absorbance value of blank (green coloured wells, Figure 4.) is subtracted from measured absorbance values of samples and standards. This step eliminates influence of buffer. To eliminate autocatalysis influence, absorbance value measured in grey wells (Figure 4.) is subtracted from absorbance values of respective samples. Enzyme activity is calculated from standard curve which correlates A_{405} of standards and concentration of product pNP. Targeted A_{405} measuring range was from 0.75-1.1 because in this narrow range, correlation of product concentration and absorbance is linear. One unit (U) corresponds to 1 mM of product (pNP) per minute.

3.7.4. Total protein quantitation – modified Bradford's protein assay

Prior to the measurement samples were diluted in H_2O_{dd} - supernatants were diluted in a range of 1:5 to 1:40 and cell lysate samples in a range of 1:10 to 1:300. According to the schedule (Figure 4.), 50 µL of each calibration standard and 50 µL of the sample dilutions were pipetted into the wells of a 96-well plate. Standards were pipetted in two replicates and samples in three technical replicates. BSA (*bovine serum albumin*) was used as standard.

Roti®–Nanoquant solution (5 x) was diluted in 4 volumes of H_2O_{dd} and 200 µL of 1 x solution was pipetted to the standards and the samples on plate. The plate was incubated for 5 minutes at room temperature. Thereafter, OD_{590} and OD_{450} were measured using software SoftMax® Pro. To calculate the protein concentration, the quotient OD_{590}/OD_{450} of each sample was compared to the calibration curve (dependence of OD_{590}/OD_{450} to protein concentration).
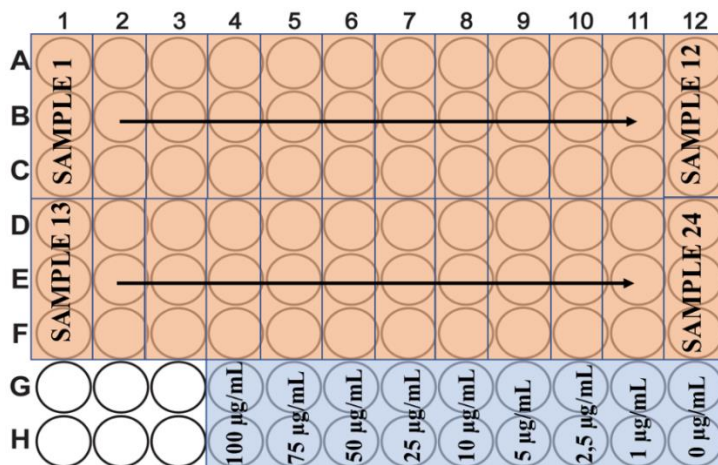
Figure 4*. Pipetting schedule for total protein test: orange colour stands for samples (pipetted in three replicates) and blue colour represents standards (pipetted in two replicates).*

3.7.5. SDS – PAGE

Protein samples (prepared in 4 x Laemmli buffer followed by boiling at 96°C for 5 min) were separated on SDS-PAGE gels. Polyacrylamide gels are composed of a separating and a stacking gel (Table 10.). First, the separation gel was poured and layered with isopropanol. It was polymerizing for 30 min at room temperature. Thereafter, isopropanol was removed, the stacking gel was poured, and a comb was inserted into the layer of stacking gel solution. It was left for 10 min to polymerize. Afterwards, the comb was removed, the gel was placed in the electrophoresis apparatus and filled with 1 x electrophoresis buffer. 8 µL of pre-stained marker and 20 µL of prepared samples were loaded and electrophoresis was performed at the

current of 20 mA for the stacking gel and of 40 mA for the separation gel. Electrophoresis is tracked by stain migration and stopped when stain reached the bottom of the plate. Gels were stained in Comassie brilliant blue solution (Table 10.) and destained in water. Both staining and destaining was performed on orbital rocking shaker. Composition of each gel and other used solutions is listed in tables below.

Table 10. Composition of polyacrylamide separating and stacking gel.

	separating gel (12,5%)	stacking gel (5%)
H_2O	1,5 mL	775 µL
1 M Tris – HCl, pH 8,8	2,8 mL	-
0,25 M Tris – HCl, pH 6,8	-	1,25 mL
Bis/Acrylamide (0,8%, 30%)	3,0 mL	425 µL
5% SDS	150 µL	50 µL
10% APS	37,5 µL	25 µL
TEMED	2,5 µL	2,5 µL

Table 11. Composition of buffers and stain solution used for SDS-PAGE.

Solution	Component	concentration
4 x Laemmli buffer, pH 6,8	bromphenol blue	200 mg/L
	dithiothreitol	200 mM
	Glycerine	200 g/L
	SDS	40 g/L
	Tris-HCl	100 mM
stain solution	80% *o*-phosphoric acid	2 % (v/v)
	ammonium sulphate	50 g/L
	Coomassie brilliant blue G-250	200 mg/L
	ethanol	10 % (v/v)
Tris-glycine electrophoresis buffer, pH 8,3	Glycine	192 mM
	SDS	1 g/L
	Tris	25 mM

4. RESULTS AND DISCUSSION

This chapter contains results obtained during flask cultivations of two different *E. coli* strains without and with pAppA plasmid. The aim of the flask cultivation was to see how transformation of cells with pAppA plasmid influence the cell growth and to see how certain deletions of the transformed selected strains influence cell growth, protein production and secretion. Strains were cultivated in larger scale, i. e. in bioreactors. Each of the strains has also kanamycin resistance, i. e. *Δkan* mutation.

4.1. FLASK CULTIVATION OF DIFFERENT *E. coli* STRAINS

4.1.1. Growth behaviour and OD$_{600}$

Figure 5 shows the OD$_{600}$ measured at nine different time points – 0h, 1h, 2h, 3h, 4h, 5h, 6h, 7h and 8h of cultivation.
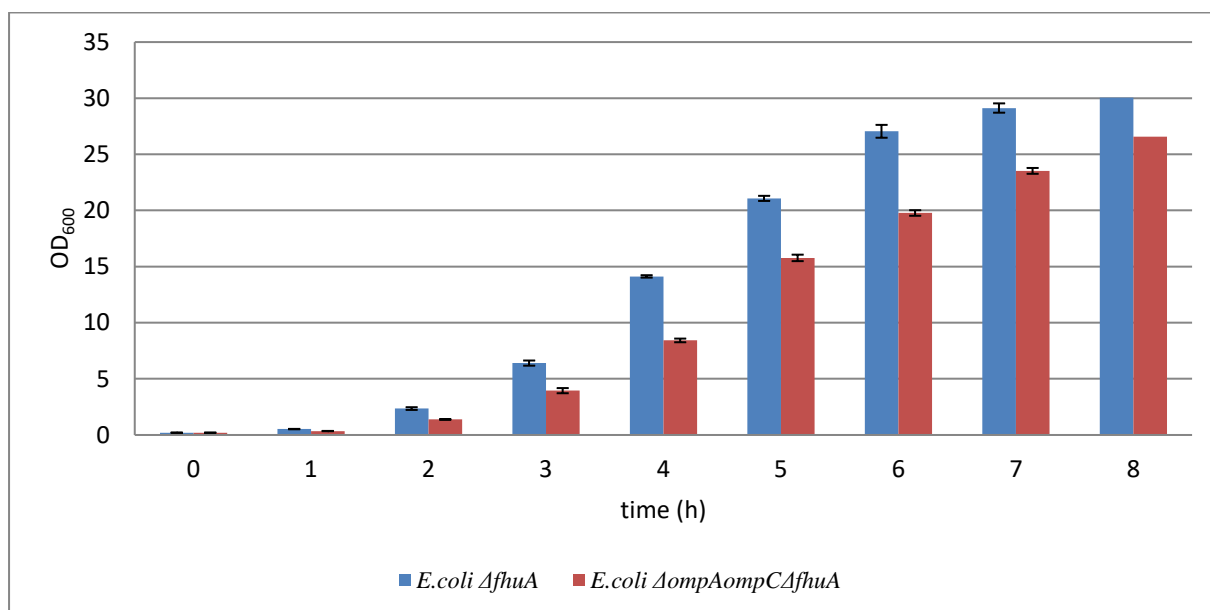
Figure 5. *Optical density of bacterial cultures. N = 2 x 2.*

At first time point (0 h) initial OD$_{600}$ of both strains is 0.2. After 8 h of cultivation, strain *E.coli ΔfhuA* has reached higher OD$_{600}$ with a value of 30.05 ± 0.41 than *E.coli ΔompAompCΔfhuA* strain with OD$_{600}$ value of 26.58 ± 0.26 (Figure 5). The highest specific growth rate for the strain *E.coli ΔfhuA* is 0.896 h^{-1}, while strain *E.coli ΔompAompCΔfhuA* has reached 0.693 h^{-1} . Generation time of the strain *E.coli ΔfhuA* is 1.11 h and for the *E.coli*

ΔompAompCΔfhuA is 1.13 h. Results and errors shown in this chart are calculated from measurement of two biological and two technical replicates, N = 2 x 2.
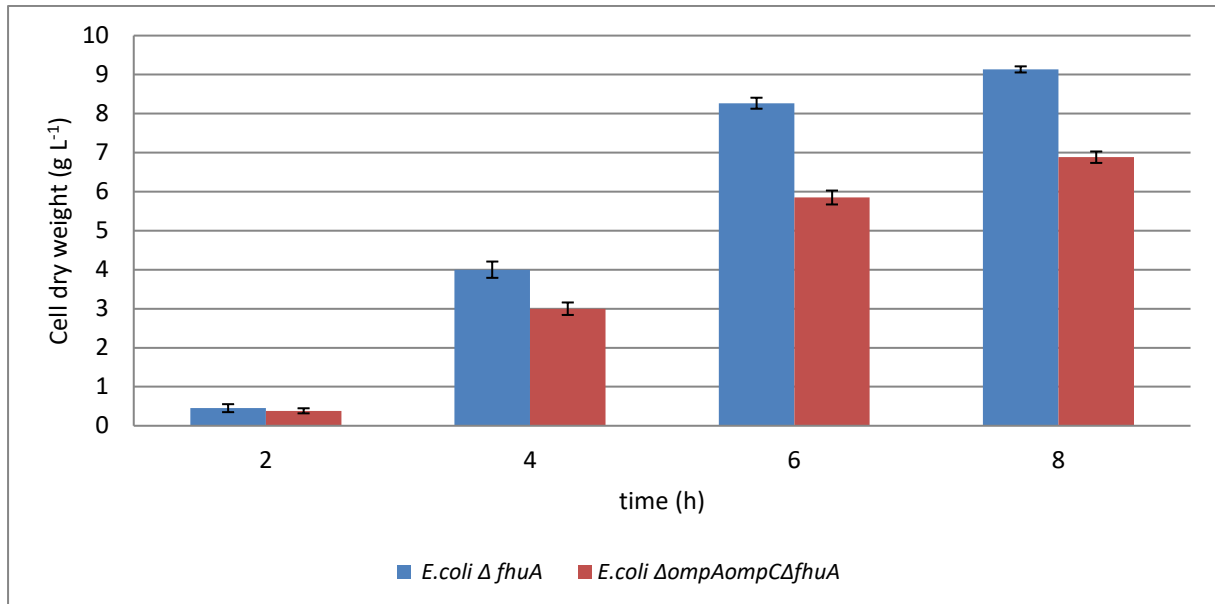
Figure 6. *Cell dry weight of bacterial cultures. N = 2 x 3.*

In 2, 4, 6, and 8 h of cultivation, cell dry weight of strain *E.coli ΔfhuA* was higher than a cell dry weight of a strain *E.coli ΔompAompCΔfhuA*, which corresponds to the OD measurements. The highest measured cell dry weight of both strains was eighth hours of cultivation, with a value of 9.13 ± 0.08 g L^{-1} for strain *E.coli ΔfhuA* while for strain *E.coli ΔompAompCΔfhuA* it is 6.88 ± 0.15 g L^{-1} (Figure 6). Results and errors shown in this chart are calculated from measurement of two biological and three technical replicates, N = 2 x 3.
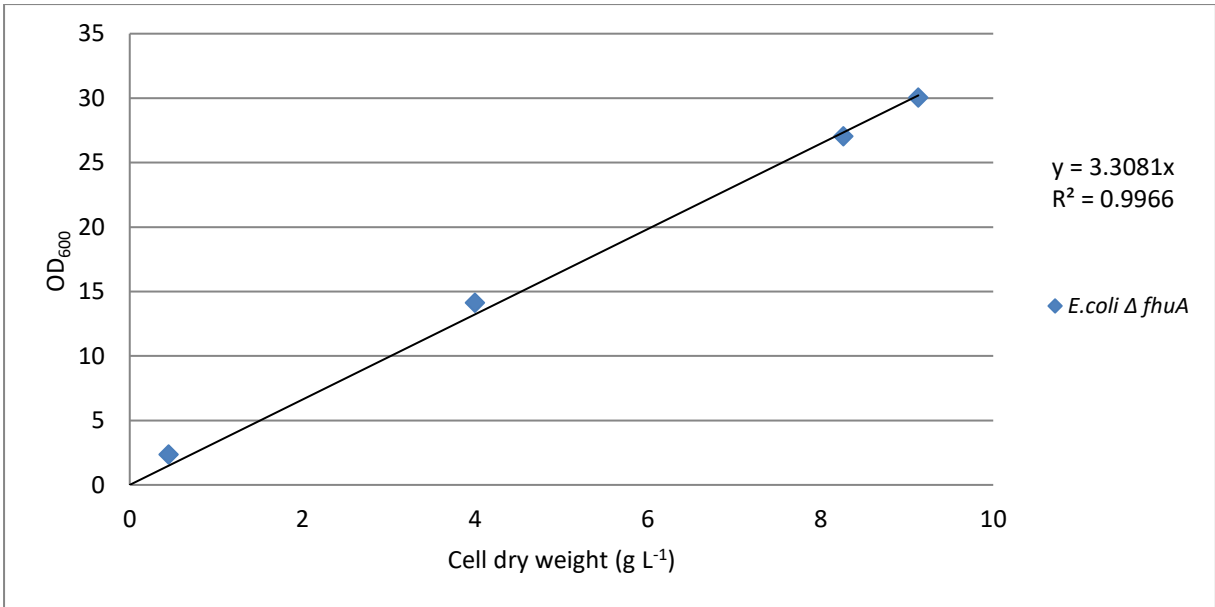
Figure 7. *Correlation of OD$_{600}$ with cell dry weight for strain E.coli ΔfhuA*

For the strain *E.coli ΔfhuA* the equation y = 3.3081x represents the correlation of cell culture optical density at 600nm with cell dry weight, with the coefficient of determination of 0.9966 (Figure 7).
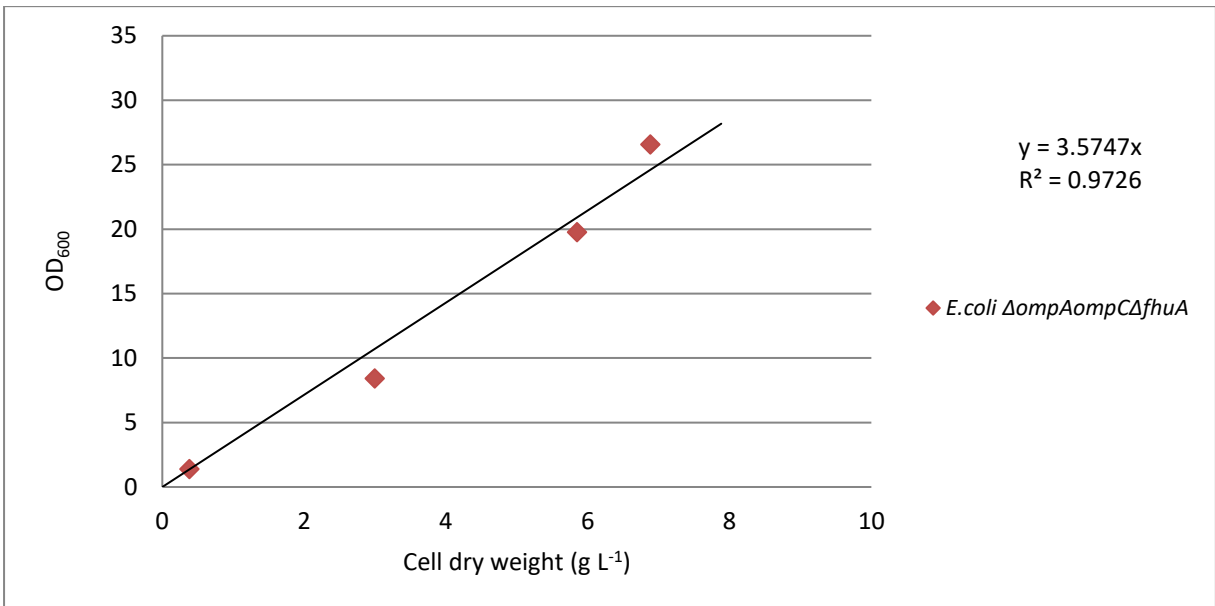
Figure 8. *Correlation of OD$_{600}$ with cell dry weight for strain E.coli ΔompAompCΔfhuA*

For the strain *E.coli ΔompAompCΔfhuA* the equation y = 3.5747x represents the correlation of cell culture optical density at 600nm with cell dry weight, with the coefficient of determination of 0.9726 (Figure 8).

.
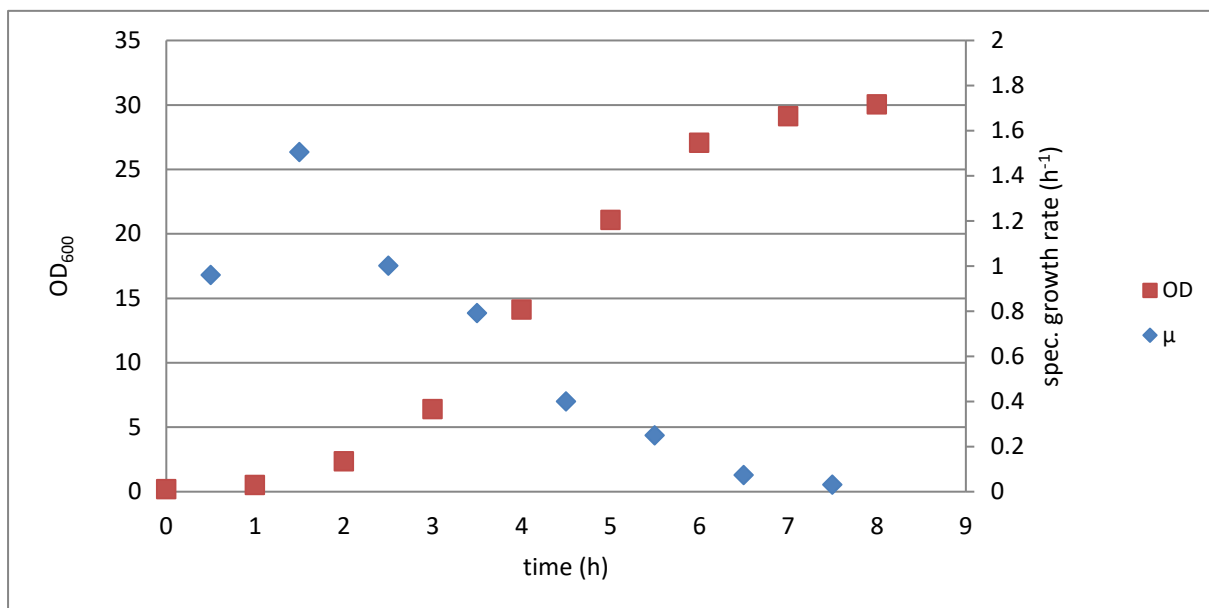
Figure 9. *Specific growth rate and OD measurements of strain E.coli ΔfhuA*

At the first time point (0.5 h) specific growth rate of strain *E.coli ΔfhuA* is lower (0.96 h^{-1}) than a specific growth rate (1.51 h^{-1}) at the second time point (1.5 h) because of the adaptation of cells to the new media. Furthermore, at the second time point (1.5 h) cells have reached the highest specific growth rate (1.51 h^{-1}) (Figure 9). Mean value of specific growth rate of strain *E.coli ΔfhuA* is 0.63 h^{-1}. Generation time of the strain is 1.11 h. Results of optical density shown in this chart are calculated from measurement of two biological and two technical replicates, N = 2 x 2.
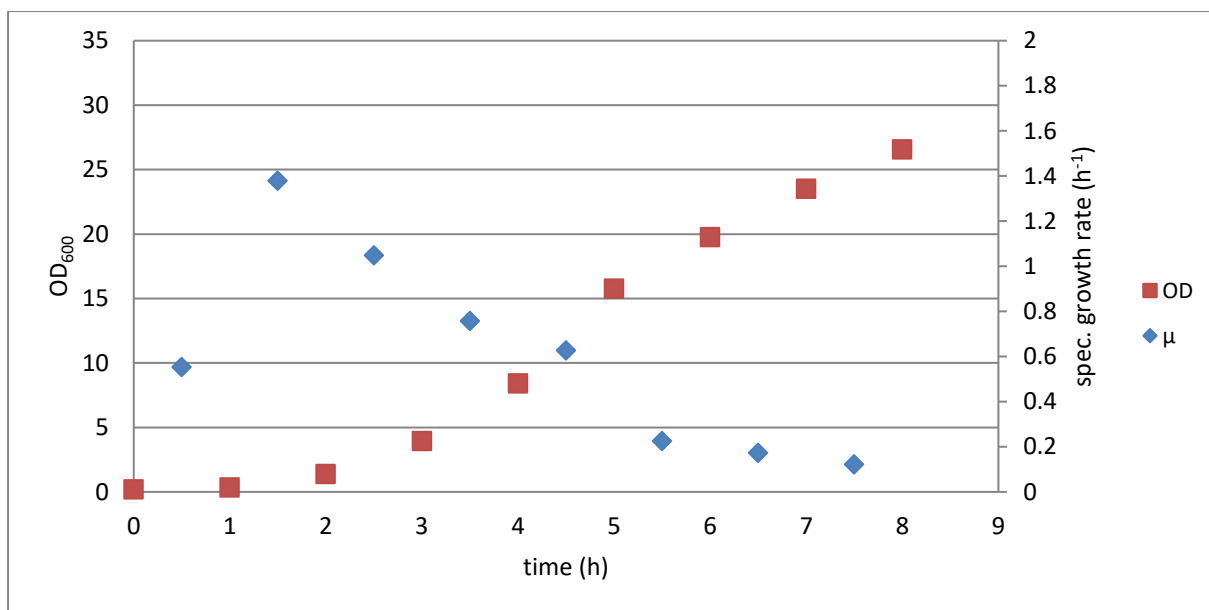
Figure 10. *Specific growth rate (μ) and OD measurements of strain E.coli ΔompAompCΔfhuA*

At the first time point (0.5 h) specific growth rate of strain *E.coli ΔompAompCΔfhuA* is lower (0.55 h^{-1}) than a specific growth rate (1.38 h^{-1}) at the second time point (1.5 h) because of the adaptation of cells to the new media. Furthermore, at the second time point (1.5 h) cells have reached the highest specific growth rate (1.38 h^{-1}) (Figure 10). Mean value of specific growth rate of strain *E.coli ΔompAompCΔfhuA* is 0.61 h^{-1}. Generation time of the strain is 1.13 h. Results of optical density shown in this chart are calculated from measurement of two biological and two technical replicates, N = 2 x 2.

4.2. FLASK CULTIVATION OF DIFFERENT *E. coli* TRANSFORMED STRAINS WITH pAppA PLASMID
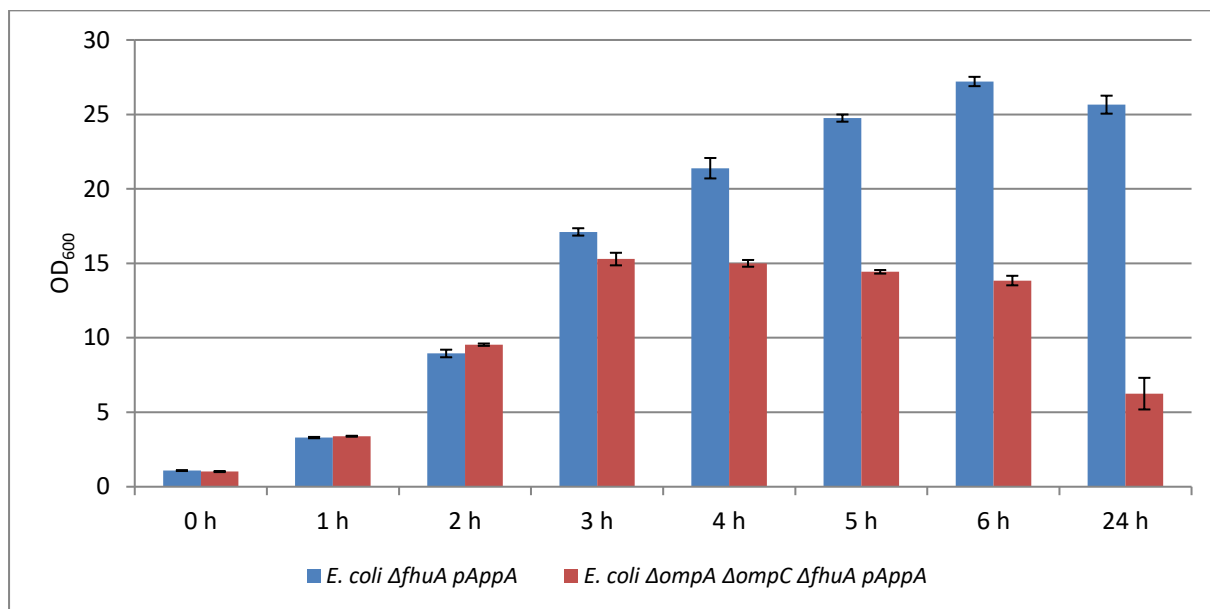
Figure 11. *Optical density of bacterial cultures measured right after induction. N = 3 x 3*

Figure 11 shows the OD_{600} measured at eight different time points – 0 h (right after induction), 1 h (one hour after induction), 2 h (two hours after induction), 3 h (three hours after induction), 4 h (four hours after induction), 5 h (five hours after induction), 6 h (six hours after induction), 24 h (twenty – four hours after induction). For strain *E. coli ΔfhuA pAppA* induction (0 h) of protein production with final concentration of 1 mM IPTG was at OD_{600} of 1.09 ± 0.03 and for strain *E.coli ΔompAompCΔfhuA pAppA* it was at OD_{600} of 1.02 ± 0.04. The strains *E. coli ΔfhuA pAppA* and *E.coli ΔompAompCΔfhuA pAppA* have reached similar OD_{600} both at the point of the induction and first hour after induction. Strain *E.coli ΔompAompCΔfhuA pAppA* has reached the highest OD_{600} of 15.29 ± 0.42 in third hour after induction after which OD_{600} has started decreasing, which indicates that cells culture have gone into death phase. For the strain *E. coli ΔfhuA pAppA* the highest measured OD_{600} of 27.21 ± 0.31 was in sixth hour after induction. Twenty – four hours after induction OD_{600} of a strain *E. coli ΔfhuA pAppA* decreases to the value of 25.66 ± 0.60.

Strain *E. coli ΔompA ΔompC ΔfhuA pAppA* grows faster with a mean value of specific growth rate of 0.638 h^{-1} (Figure 13.), while mean value of specific growth rate for strain *E.coli ΔfhuA*

pAppA is 0.635 h^{-1} (Figure 12). Additionally, *E.coli ΔompAompCΔfhuA pAppA* strain has a shorter generation time (1.087 h) than a strain *E.coli ΔfhuA* (1.091 h). The highest specific growth rate of a strain *E.coli ΔfhuA pAppA* is 0.927 h^{-1} and for the strain *E.coli ΔompAompCΔfhuA pAppA* it is 0.916 h^{-1}.

It could be that the triple knock out strain *E.coli ΔompAompCΔfhuA pAppA* grows faster because the outer membrane of the strain is more permeabilized so the velocity of substrate transport into the cell could be higher. On the other hand, it could be that with more permeabilized outer membrane, the cells are less stable because they are losing necessary substances out of the periplasm and therefore cells culture skipped stationary phase and went into death phase immediately.

Influence of induction between cells which are transformed with plasmid and those which are not, manifests in cell culture optical density measurements and the highest specific growth rate. Strain *E. coli ΔfhuA pAppA* has reached lower highest measured OD$_{600}$ of 27.21 ± 0.31 in sixth hour after induction (Figure 11) than a strain *E. coli ΔfhuA* after 8h of cultivation with a highest measured OD$_{600}$ of 30.05 ± 0.41 (Figure 5). The highest specific growth rate of *E. coli ΔfhuA* is 0.896 h^{-1}, while for *E. coli ΔfhuA pAppA* the highest specific growth rate is 0.927 h^{-1}. However, influence of induction was even greater for the strain *E. coli ΔompA ΔompC ΔfhuA pAppA* which has reached highest OD$_{600}$ of 15.29 ± 0.42 in third hour after induction, after which cells went into death phase (Figure 11), than a strain *E. coli ΔompA ΔompC ΔfhuA* which has reached OD$_{600}$ of 26.58 ± 0.26 after 8h of cultivation (Figure 5). The highest specific growth rate of a strain *E. coli ΔompA ΔompC ΔfhuA* is 0.693 h^{-1}, while for *E. coli ΔompA ΔompC ΔfhuA pAppA* the highest specific growth rate is 0.916 h^{-1}.
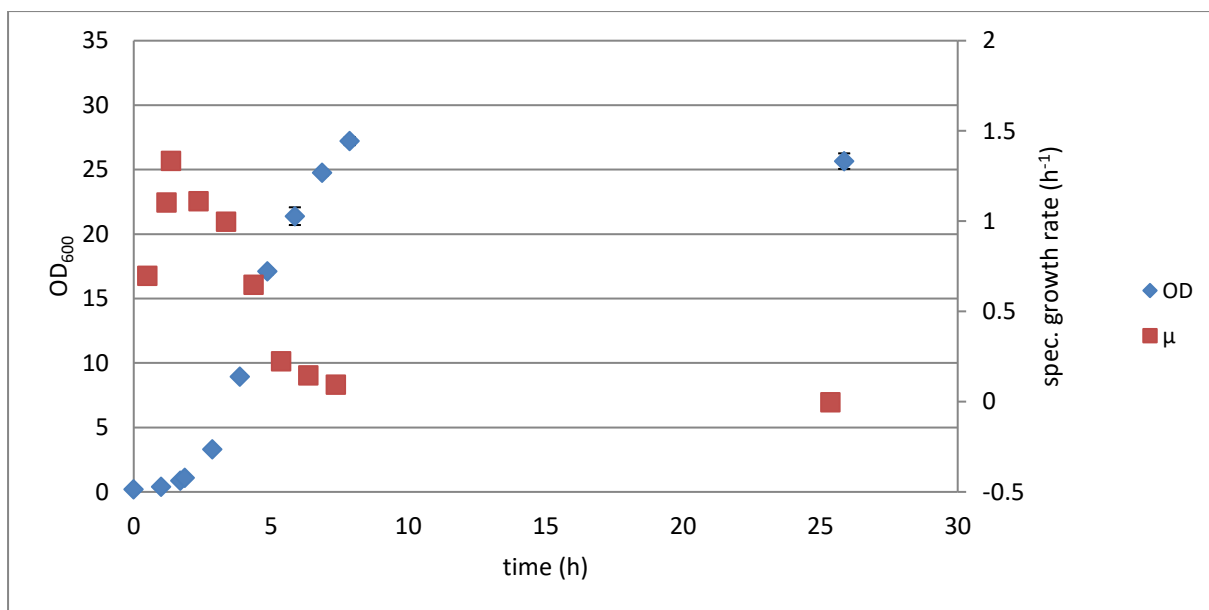
Figure 12. *Specific growth rate (μ) and OD measurements of strain E.coli ΔfhuA with pAppA plasmid.*

At the first (0.5 h) and the second (1.2 h) time points, specific growth rates of strain *E.coli ΔfhuA pAppA* are lower (0.70 h^{-1} and 1.10 h^{-1}) than a highest specific growth rate (1.33 h^{-1}) at third time point (1.37 h) because of the adaption of cells to the new media (Figure 12). Mean value of specific growth rate of strain *E.coli ΔfhuA pAppA* is 0.64 h^{-1}. Generation time of the strain is 1.09 h. Results and errors shown in this chart for optical density, are calculated from measurement of three biological and three technical replicates, N = 3 x 3.
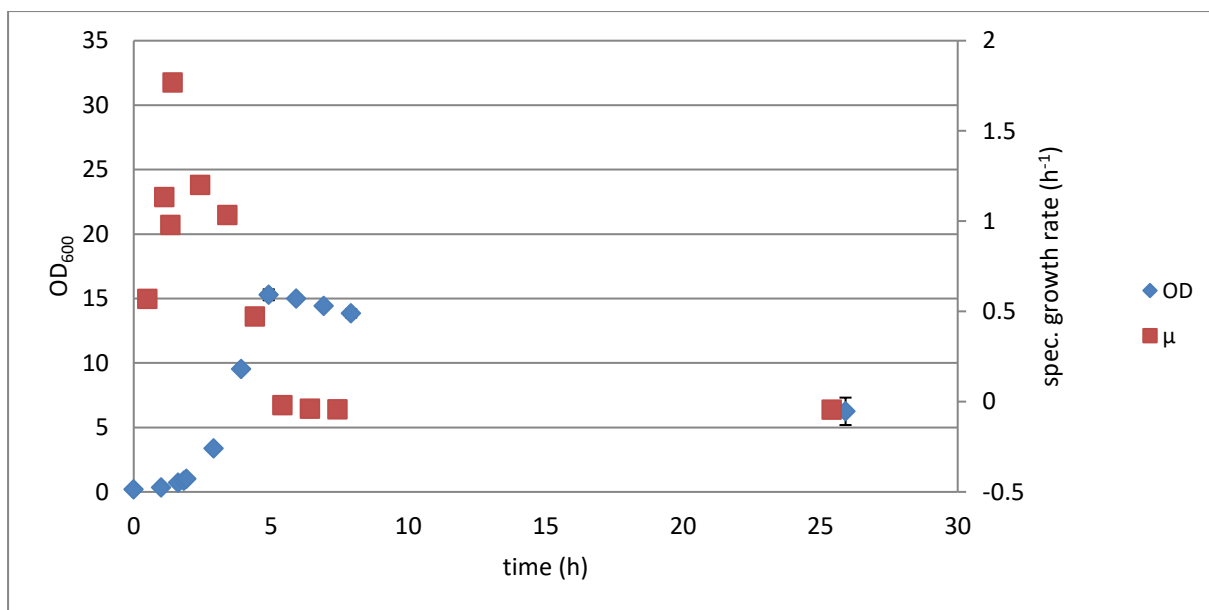
Figure 13. *Specific growth rate (μ) and OD measurements of strain E. coli ΔompA ΔompC ΔfhuA with pAppA plasmid.*

The highest specific growth rate is 1.77 h^{-1} at 1.42 h of cultivation. After reaching the highest measured OD_{600} of 15.29 ± 0.42 at third hour after induction, cells culture went into death phase. Therefore, specific growth rate of the last four measurements is below 0 h^{-1} (Figure 13). Mean value of specific growth rate of strain *E. coli ΔompA ΔompC ΔfhuA pAppA* is 0.64 h^{-1}. Generation time of a strain is 1.09 h. Results and errors shown in this chart for optical density, are calculated from measurement of three biological and three technical replicates, N = 3 x 3.

By using the equation y = 3.3081x which represents the correlation of cells optical density at 600nm with cell dry weight for the strain *E.coli ΔfhuA* with the coefficient of determination of 0.9966 (Figure 7), cell dry weight has been calculated for the strain *E.coli ΔfhuA pAppA*. Results have been shown in Table 12.

Table 12. *Cell dry weight of a strain E.coli ΔfhuA pAppA*

Time (h)	OD$_{600}$	Cell dry weight (g L^{-1})
0	0.2 ± 0.00	0.06 ± 0.00
1	0.40 ± 0.01	0.12 ± 0.00
1.7	0.87 ± 0.00	0.26 ± 0.00
1.87	1.09 ± 0.03	0.33 ± 0.00
2.87	3.30 ± 0.04	1.00 ± 0.01
3.87	8.95 ± 0.25	2.70 ± 0.08
4.87	17.11 ± 0.25	5.17 ± 0.07
5.87	21.39 ± 0.69	6.47 ± 0.21
6.87	24.76 ± 0.24	7.48 ± 0.07
7.87	27.21 ± 0.31	8.23 ± 0.09
25.87	25.66 ± 0.60	7.76 ± 0.18

By using the equation y=3.5747x which represents the correlation of cells optical density at 600nm with cell dry weight for the strain *E.coli ΔompAompCΔfhuA* with the coefficient of determination of 0.9726 (Figure 8), cell dry weight has been calculated for the strain *E.coli ΔompAompCΔfhuA pAppA*. Results have been shown in Table 13.

Table 13. *Cell dry weight of a strain E.coli ΔompAompCΔfhuA pAppA*

Time (h)	OD$_{600}$	Cell dry weight (g L^{-1})
0	0.2 ± 0.00	0.06 ± 0.00
1	0.35 ± 0.00	0.10 ± 0.00
1.62	0.71 ± 0.00	0.20 ± 0.00
1.83	0.88 ± 0.00	0.25 ± 0.00
1.92	1.02 ± 0.04	0.29 ± 0.01
2.92	3.39 ± 0.03	0.95 ± 0.00
3.92	9.54 ± 0.08	2.67 ± 0.02
4.92	15.29 ± 0.42	4.28 ± 0.12
5.92	15 ± 0.23	4.20 ± 0.06
6.92	14.43 ± 0.12	4.04 ± 0.03
7.92	13.84 ± 0.32	3.87 ± 0.09
25.92	6.25 ± 1.06	1.75 ± 0.30

4.2.2. Protein secretion

Protein concentration in the supernatant was determined. Results of modified Bradford test described in chapter Materials and methods are shown on Figure 14 and Figure 15.
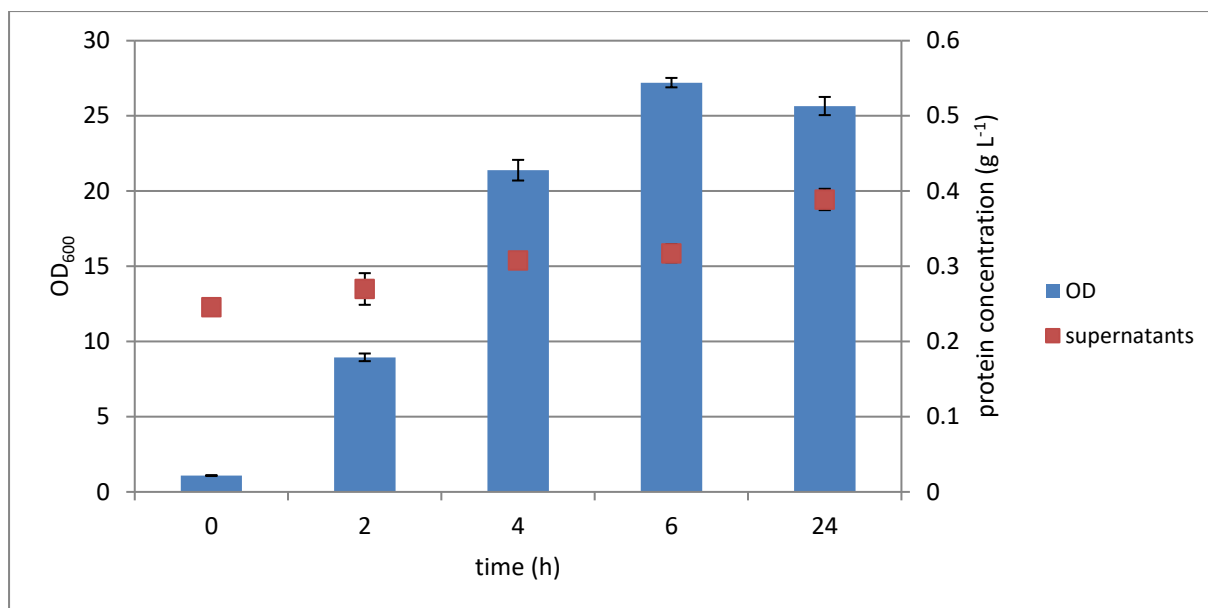
Figure 14. *Optical density and protein concentration in supernatants of E. coli ΔfhuA pAppA. N = 3 x 3.*

Figure 14 shows the OD_{600} and protein concentration in supernatants measured at five different time points – 0 h (right after induction), 2 h (two hours after induction), 4 h (four hours after induction), 6 h (six hours after induction), 24 h (twenty – four hours after induction). It can be noticed that as well as OD_{600} increases over the time, protein concentration in supernatant increases too. The highest protein concentration in supernatant of 0.39 ± 0.01 g L^{-1} is reached at twenty – fourth hour after induction and it is more than 1.5x higher than at the point of induction, which is in correlation with the decrease of OD_{600} thus indicating cell lysis.
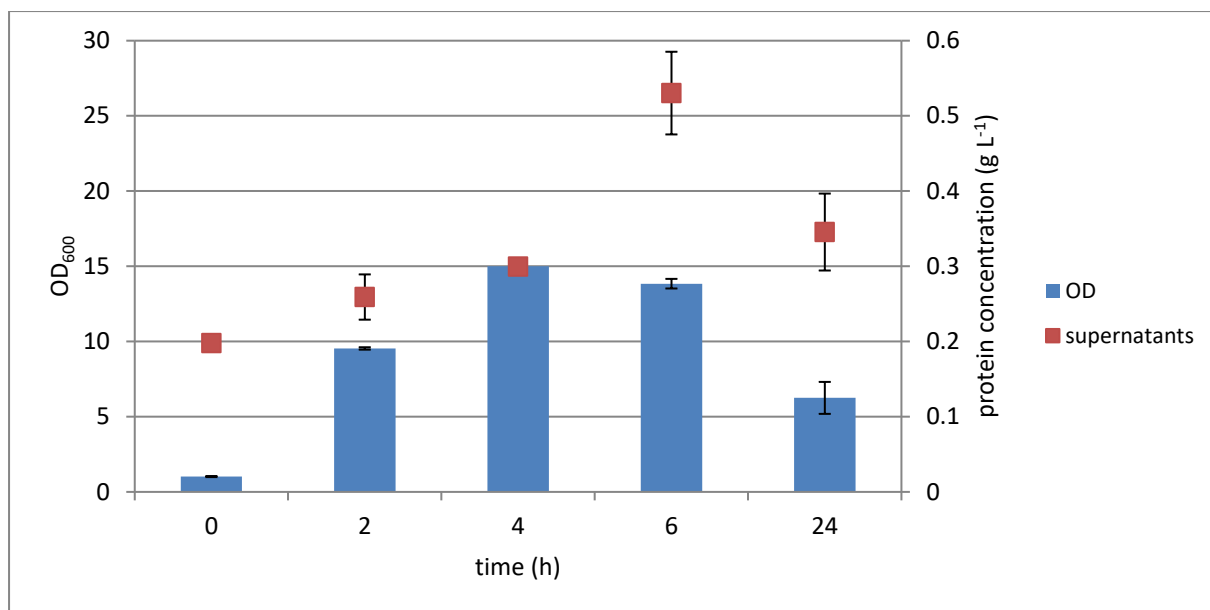
Figure 15. *Optical density and protein concentration in supernatants of E. coli*
ΔompAompCΔfhuA pAppA. N = 3 x 3

Figure 15 shows the OD_{600} and protein concentration in supernatants measured at five
different time points – 0 h (right after induction), 2 h (two hours after induction), 4 h (four
hours after induction), 6 h (six hours after induction), 24 h (twenty – four hours after
induction). With increase of OD_{600} protein concentration in supernatants also increases at the
point of induction, second and fourth hour after induction. However, in sixth and twenty –
fourth hour after induction OD_{600} decreases while protein concentration is supernatants
increases presumably because of cell lysis. Because protein concentration in twenty – fourth
hour is lower (0.35 ± 0.05 g L^{-1}) than in sixth hour (0.53 ± 0.05 g L^{-1}) it could indicate that
there has been made mistake either with sampling or with the method.
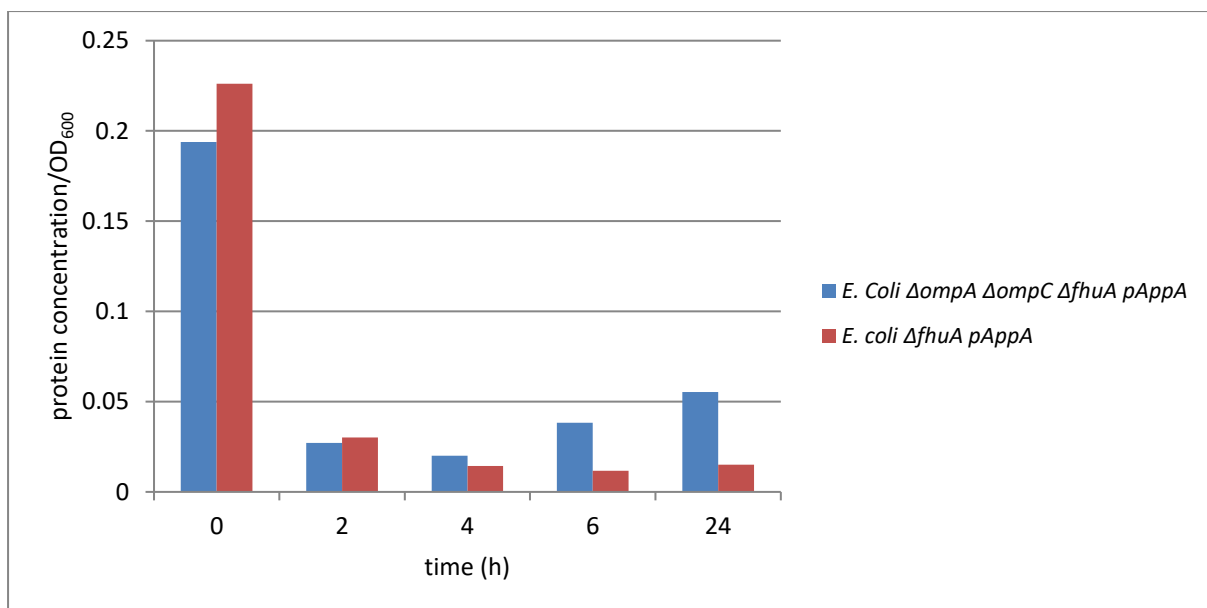
Figure 16. *Normalized protein concentration comparison in supernatant of two different E. coli strains.*

In Figure 16 bars represent the protein concentration in supernatants normalized to the OD_{600} of the respective strains. The highest normalized protein concentration in supernatant of both strains can be noticed at the point of induction. This could be due to the inoculation, since it is possible that lysis of some cells occurred in preculture because in the starter culture, cells can be in dissimilar metabolic states (Huber *et al.,* 2009; Rosano and Ceccarelli, 2014). At the point of induction and second hour after induction, normalized protein concentration of *E. coli ΔfhuA pAppA* is higher than *E. coli ΔompAompCΔfhuA pAppA*. From fourth hour after induction until the end of cultivation, *E. coli ΔompAompCΔfhuA pAppA* has higher normalized protein concentration. Twenty – fourth hour after induction normalized protein concentration of *E. coli ΔompAompCΔfhuA pAppA* is 3.65 times higher than *E. coli ΔfhuA pAppA*, but it is important to accentuate that OD_{600} of *E. coli ΔompAompCΔfhuA pAppA* started decreasing in fourth hour after induction.

4.2.3. Enzyme activity

Table 14 contains the results of enzyme assay preformed as described in the chapter Materials and methods. Enzyme activity in supernatants of different strains are shown as total activity and as activity normalized to OD_{600}.

***Table 14.*** *Enzyme assay and OD_{600} results for tested E. coli strains*

Strain	time after induction (h)	OD_{600}	total enzyme activity ($U\ mL^{-1}$) in supernatant	normalized enzyme activity ($U\ mL^{-1}\ OD^{-1}$) in supernatant	volumetric productivity ($U\ mL^{-1}\ h^{-1}$)
E. coli ΔfhuA pAppA	2	8.95 ± 0.25	0.02 ± 0.00	0.003 ± 0.000	-
	4	21.39 ± 0.69	0.12 ± 0.01	0.006 ± 0.001	0.050
	6	27.21 ± 0.31	0.18 ± 0.01	0.007 ± 0.001	0.040
	24	25.66 ± 0.6	1.58 ± 0.31	0.062 ± 0.007	0.071
E. Coli ΔompA ΔompC ΔfhuA pAppA	0	1.02 ± 0.02	0.04 ± 0.01	0.041 ± 0.006	-
	2	9.54 ± 0.25	0.07 ± 0.01	0.007 ± 0.002	0.013
	4	15 ± 0.59	0.90 ± 0.11	0.060 ± 0.020	0.213
	6	13.84 ± 0.36	1.99 ± 0.24	0.144 ± 0.040	0.324

For the strain *E. coli ΔfhuA* pAppA at the point of the induction and for the strain *E. coli ΔompA ΔompC ΔfhuA* pAppA at twenty – fourth hour after induction, enzyme activity in the supernatant could not have been measured due to the too low product concentration. All measured samples of strains had too high dilutions, thus eluding the targeted A_{405} that has measuring range from 0.75 – 1.1 where correlation of product concentration and absorbance is linear. Because of that, these results are not reliable. Furthermore, errors are high due to different cell growth in each of three biological replicates.

As can be seen in the table above, there are differences in the enzyme activity between the tested strains. The highest total enzyme activity can be noticed for a strain *E. coli ΔompA ΔompC ΔfhuA* pAppA at sixth hour after induction (1.99 ± 0.24 U mL^{-1}), while for the strain *E. coli ΔfhuA* pAppA it is at twenty - fourth hour after induction (1.58 ± 0.31 U mL^{-1}). These obtained results match the protein concentration test (Figure 14 and 15). There is influence of triple knock out (*E. coli ΔompA ΔompC ΔfhuA* pAppA) compared with the single knock out (*E. coli ΔfhuA* pAppA) in the growth and in total protein concentration in supernatants (Figure 10 and Figure 11) while the total enzyme activity in supernatants of both strains is quite similar which could mean that there is not more enzyme in the periplasm. Similar total enzyme activity in supernatants in both strains shows that there is similar amount of enzyme in supernatants and that knock out system for this specific enzyme might not limit the secretion. Because the same amount of enzyme is produced, the amount of the enzyme is not high enough to see the difference in secretion and hence triple knock out does not show better secretion performance.

Higher volumetric productivity has been obtained for strain *E. coli ΔompA ΔompC ΔfhuA* pAppA at sixth hour after induction (0.324 U mL^{-1} h^{-1}) compared with the strain *E. coli ΔfhuA* pAppA at twenty - fourth hour after induction (0.071 U mL^{-1} h^{-1}). Since the total enzyme activity in supernatants of both strains is quite similar, none of the strains does not show better secretion performance hence higher volumetric productivity is due to higher growth rate of a strain *E. coli ΔompA ΔompC ΔfhuA* pAppA (Figure 13) compared with growth rate of a strain *E. coli ΔfhuA* pAppA (Figure 12). Because of higher growth rate, the enzyme is secreted earlier and therefore *E. coli ΔompA ΔompC ΔfhuA* pAppA shows higher volumetric productivity.
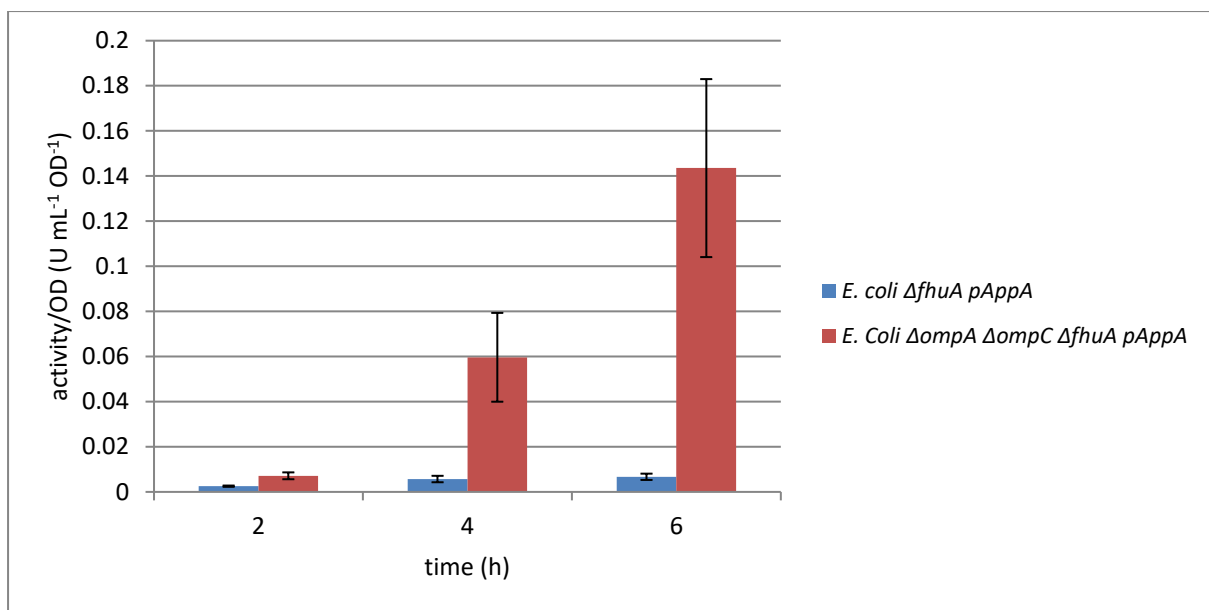
Figure 17. *Normalized activity comparison in supernatants of two different E. coli strains.*
*N= 3 x 3*

The OD_{600} must also be considered for further assessment of strains. The lower the cell
density, the lower is the number of cells that potentially secrete. The activity must therefore
be normalized to the OD_{600}. This is shown in Table 14 and Figure 17. The bars represent the
activity of phytase normalized to the OD_{600} of respective strain. Two hours after induction
higher normalized activity of supernatant is noticed for strain *E. coli ΔompA ΔompC ΔfhuA*
pAppA $(0.007 \pm 0.002$ U mL^{-1} OD$^{-1})$ than for strain *E. coli ΔfhuA* pAppA $(0.003 \pm 0.000$ U
mL^{-1} OD$^{-1})$. Fourth and sixth hour after induction, the strain *E. coli ΔompA ΔompC ΔfhuA*
pAppA has higher normalized activity of supernatant than *E. coli ΔfhuA* pAppA, but it is
important to accentuate that strain *E. coli ΔompA ΔompC ΔfhuA* pAppA showed lower cell
growth (Table 14).

4.2.3. SDS – PAGE

The following figures 18 – 26 are showing SDS-PAGE gels of supernatant and total cell culture of the tested strains at five measuring time points: 0 h, 2 h, 4 h, 6 h and 24 h. MW of phytase is expected to be around 45 kDa.
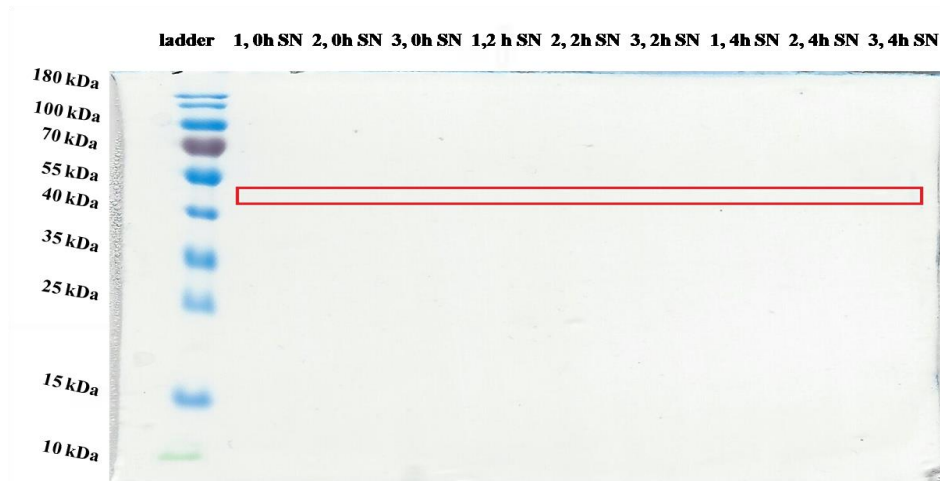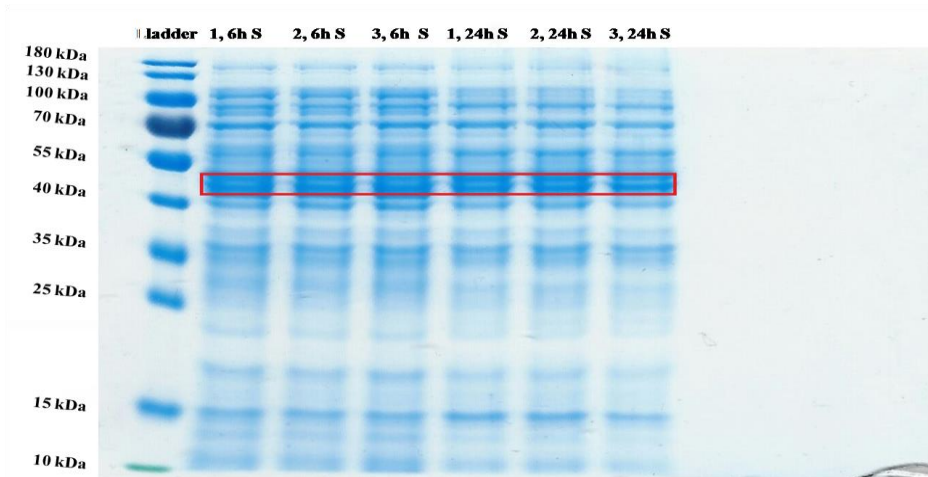

Figure 18. *SDS-PAGE, E. coli ΔfhuA pAppA. 1, 2 and 3 represent the number of flasks. 0h, 2h and 4h stand for time after induction samples were taken at. SN stands for supernatant. Red box shows phytase band.*
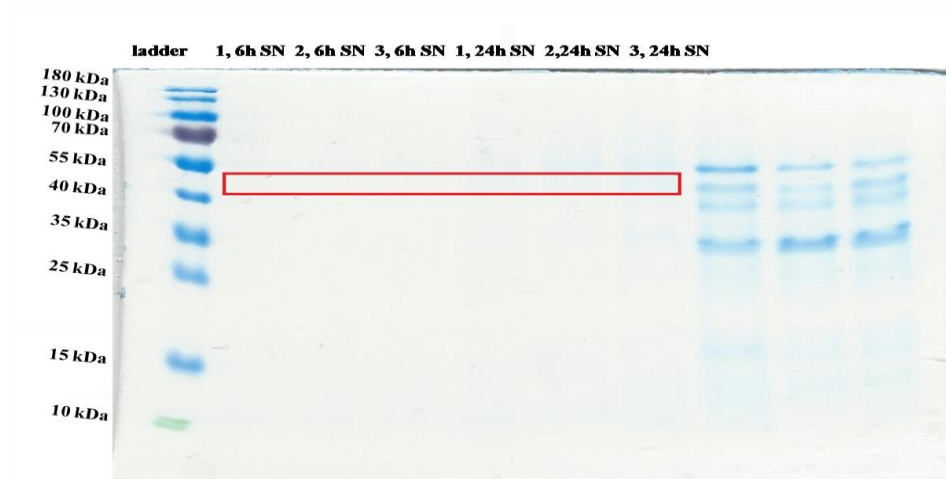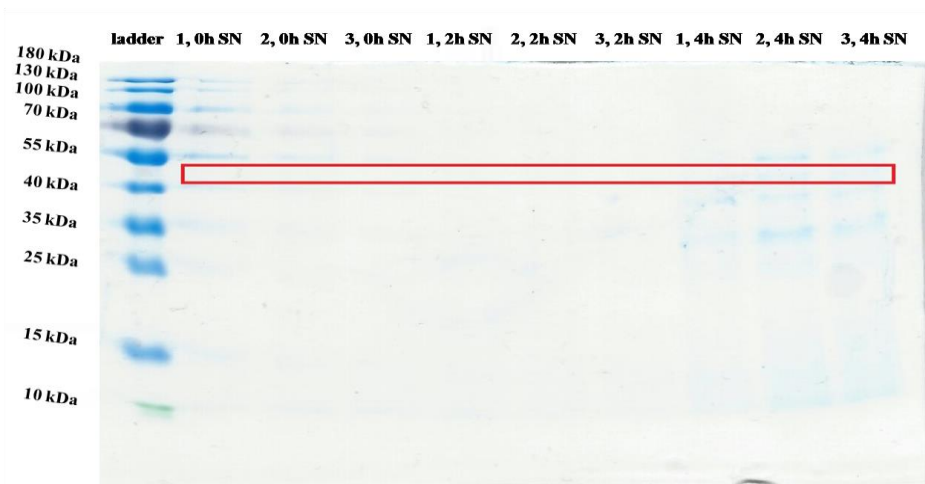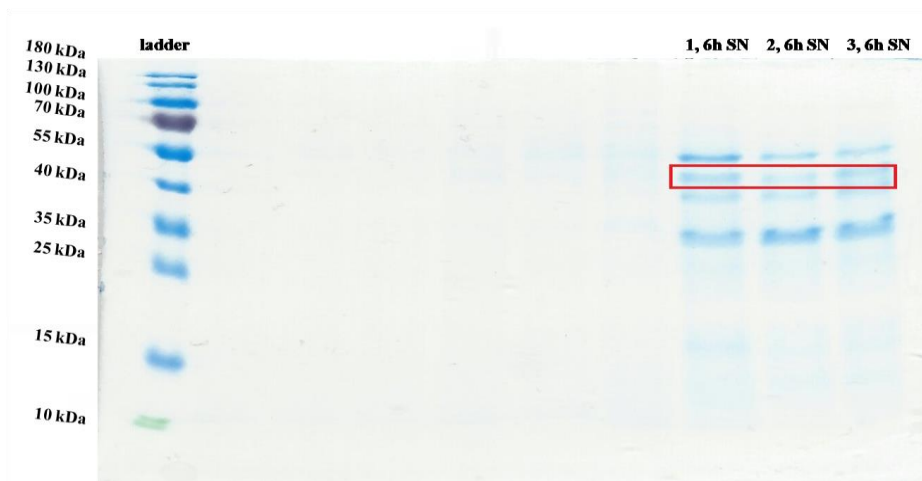

Figure 19. *SDS-PAGE, E. coli ΔfhuA pAppA. 1, 2 and 3 represent the number of flasks. 6h and 24h stand for time after induction samples were taken at. SN stands for supernatant. Red box shows phytase band.*
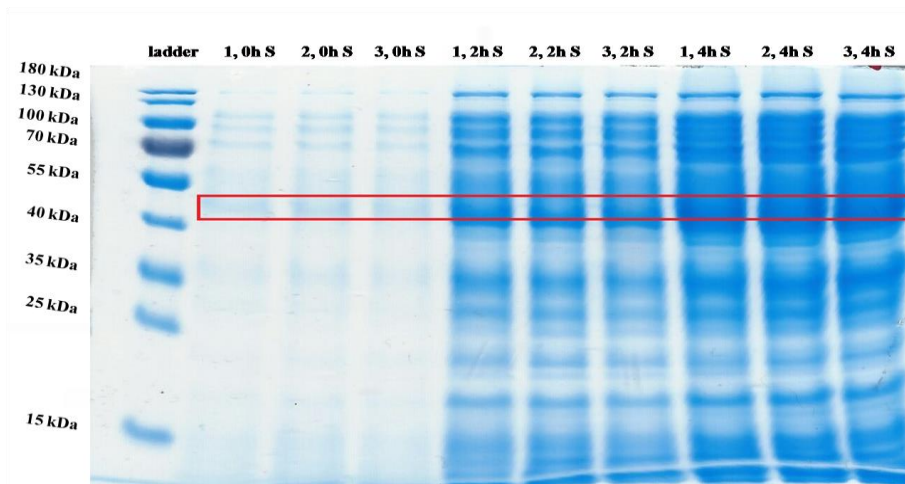
Figure 20. *SDS-PAGE, E. coli ΔfhuA pAppA. 1, 2 and 3 represent the number of flasks. 0h, 2h and 4h stand for time after induction samples were taken at. S stands for cell lysate and supernatant sample together. Red box shows phytase band.*
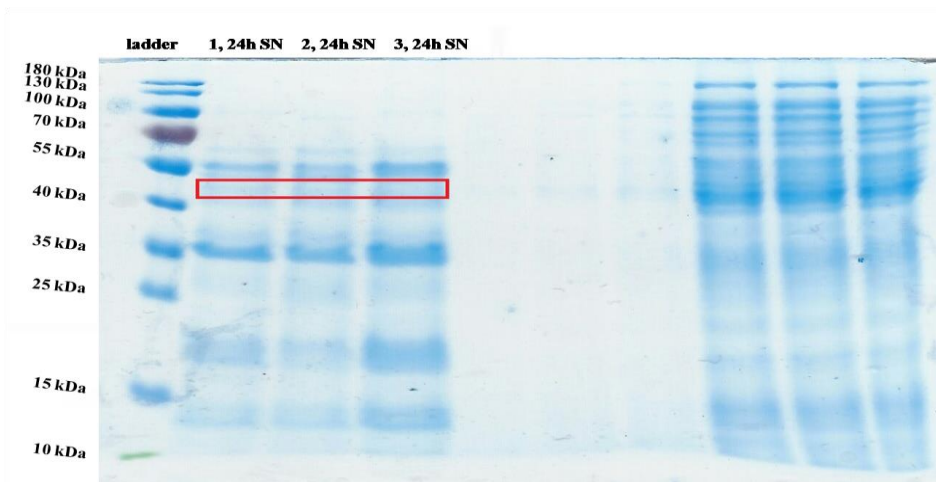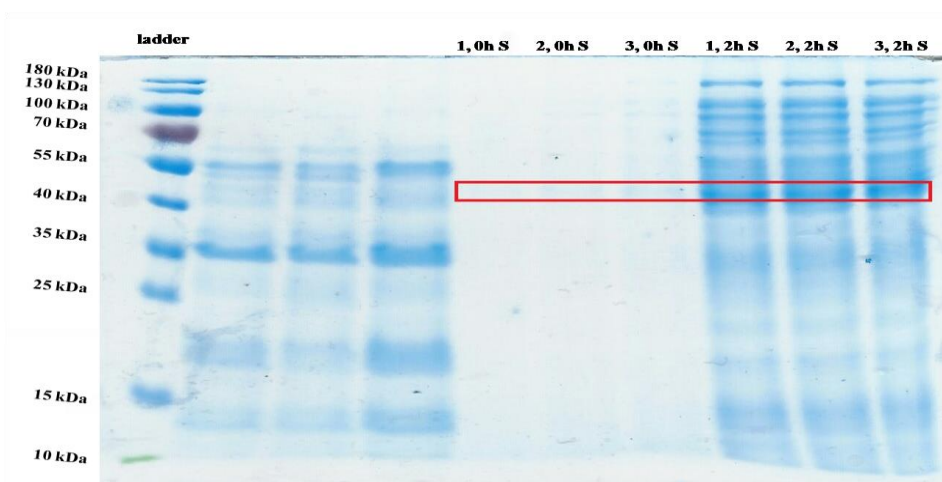

Figure 21. *SDS-PAGE, E. coli ΔfhuA pAppA. 1, 2 and 3 represent the number of flasks. 6h and 24h stand for time after induction samples were taken at. S stands for cell lysate and supernatant sample together. Red box shows phytase band.*

Figure 22. *SDS-PAGE, E. coli ΔompA ΔompC ΔfhuA pAppA. 1, 2 and 3 represent the number of flasks. 0h, 2h and 4h stand for time after induction samples were taken at. SN stands for supernatant. Red box shows phytase band.*
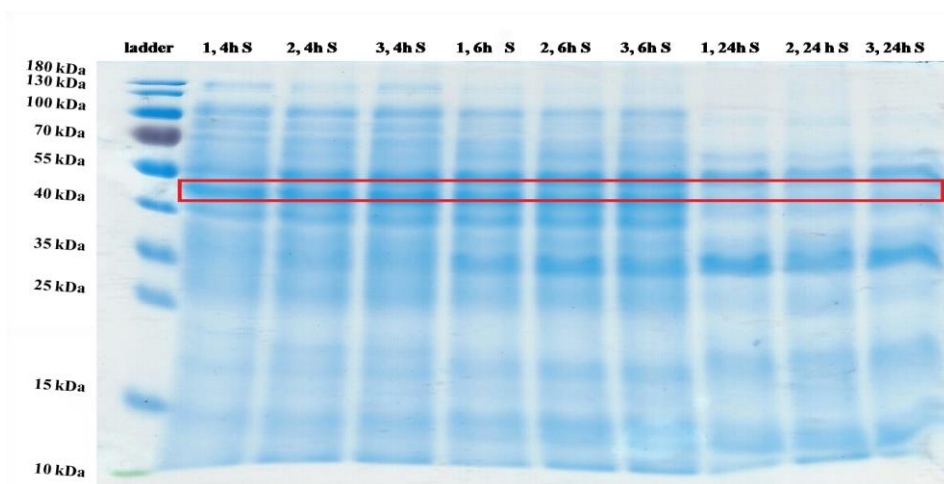

Figure 23. *SDS-PAGE, E. coli ΔompA ΔompC ΔfhuA pAppA. 1, 2 and 3 represent the number of flasks. 6h stand for time after induction samples were taken at. SN stands for supernatant. Red box shows phytase band.*

Figure 24. *SDS-PAGE, E. coli ΔompA ΔompC ΔfhuA pAppA. 1, 2 and 3 represent the number of flasks. 24h stand for time after induction samples were taken at. SN stands for supernatant. Red box shows phytase band.*

Figure 25. *SDS-PAGE, E. coli ΔompA ΔompC ΔfhuA pAppA. 1, 2 and 3 represent the number of flasks. 0h and 2h stand for time after induction samples were taken at. S stands for cell lysate and supernatant sample together. Red box shows phytase band.*

Figure 26. *SDS-PAGE, E. coli ΔompA ΔompC ΔfhuA pAppA. 1, 2 and 3 represent the number of flasks. 4h, 6h and 24h stand for time after induction samples were taken at. S stands for cell lysate and supernatant sample together. Red box shows phytase band.*

SDS – PAGE is used as a confirmation that there is secreted target protein in the nutrient medium and it can provide information whether there is a contamination with other proteins. An increased permeability of the cell wall is supposed to increase the secretion of the target protein, but it also enhances release of the other periplasmic proteins to the nutrient medium thus leading to contamination. With the signal sequence being cleaved, protein AppA has molecular weight of approximately 45 kDa (Dassa *et al.,* 1980).

In supernatant samples of strain *E. coli ΔfhuA* pAppA phytase band cannot be seen in almost all samples, except in sample taken at twenty – four hour where it is barely visible (Figure 18 and Figure 19) what matches with the highest obtained result of protein concentration test and enzyme activity test for the respective sample (Figure 14 and Table 14). The absence of the phytase band, MW of 45 kDa, in supernatant sample of this strain might be due to too small total amount of produced protein. Phytase band can be seen in all cell lysate samples of the reference strain, whereas numerous proteins stained in the gel. In the second and fourth hour after induction band is more distinct, as well as in sixth and twenty – fourth hour after induction (Figure 20 and Figure 21). It can be interpreted as this strain is having a good phytase production ability, but poor protein secretion ability.

In supernatants of strain *E. coli ΔompA ΔompC ΔfhuA* pAppA phytase band cannot be seen in at the point of induction, second and fourth hour after induction (Figure 22), while it can be clearly seen in sixth (Figure 23) and twenty – fourth hour after induction (Figure 24). Band is more distinct in supernatant sample taken at sixth rather than twenty – fourth hour, what supports result of protein concentration test (Figure 15) and enzyme assay (Table 14) since enzyme activity of supernatant sample taken at twenty – fourth hour could not be measured due to the too low product concentration. In cell lysate, phytase band is not visibly at the point of induction (Figure 25) but visibility of the phytase band on SDS-PAGE increases over the time (Figure 26). However, it can be noticed that phytase band is less visible at twenty – fourth hour after induction due to the decrease of optical density.

4.3. BIOREACTOR CULTIVATION

4.3.1. Bioreactor cultivation of *Escherichia coli ΔfhuA* **pAppA**

E. coli ΔfhuA pAppA was cultivated in 5 L bioreactor in TB medium under conditions described before in chapter Batch cultivation. Samples for measuring enzyme activity and determining protein concentration as well as for SDS-PAGE were taken 0, 2, 4, 6, 8, 12, 16, 20 and 24 hours after induction. Enzyme activity and protein concentration were determined in supernatant and in cell lysate.
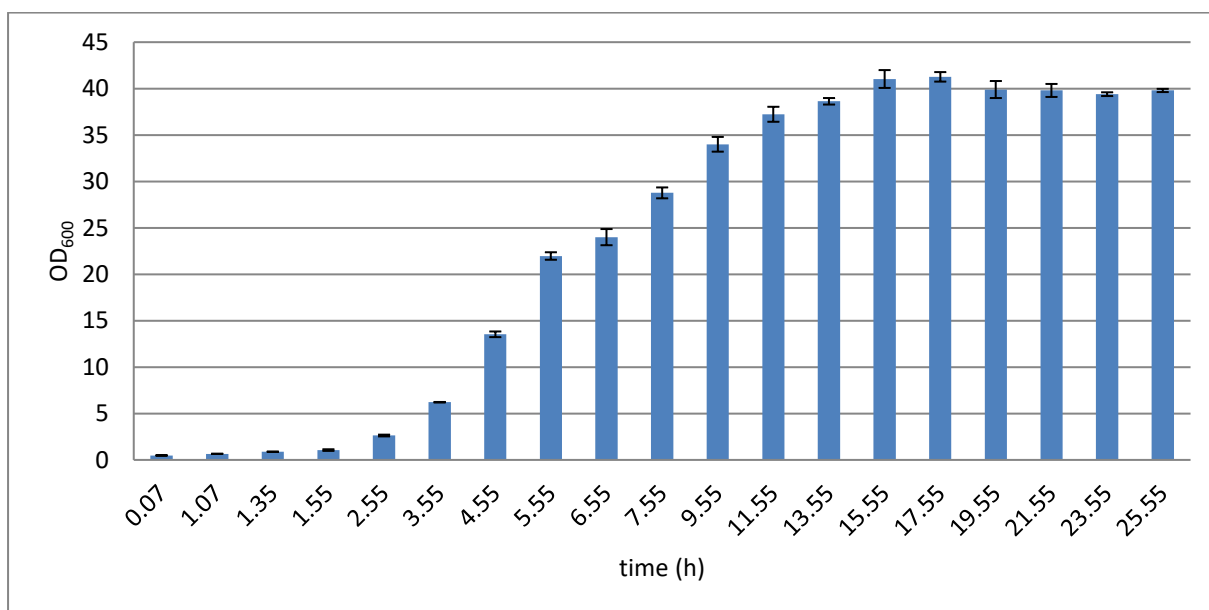
Figure 27. *Growth curve of E. coli ΔfhuA pAppA. Moment of induction was at 1.55 h. N = 1 x 3.*
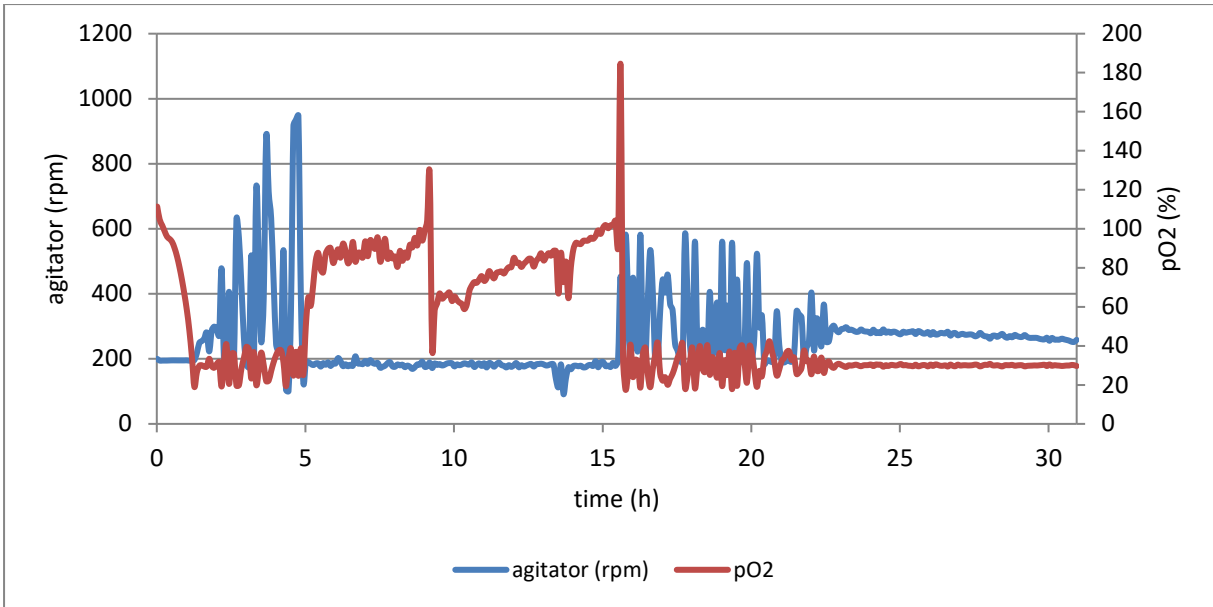
Figure 28. *Parameters of cultivation of E. coli ΔfhuA pAppA.*
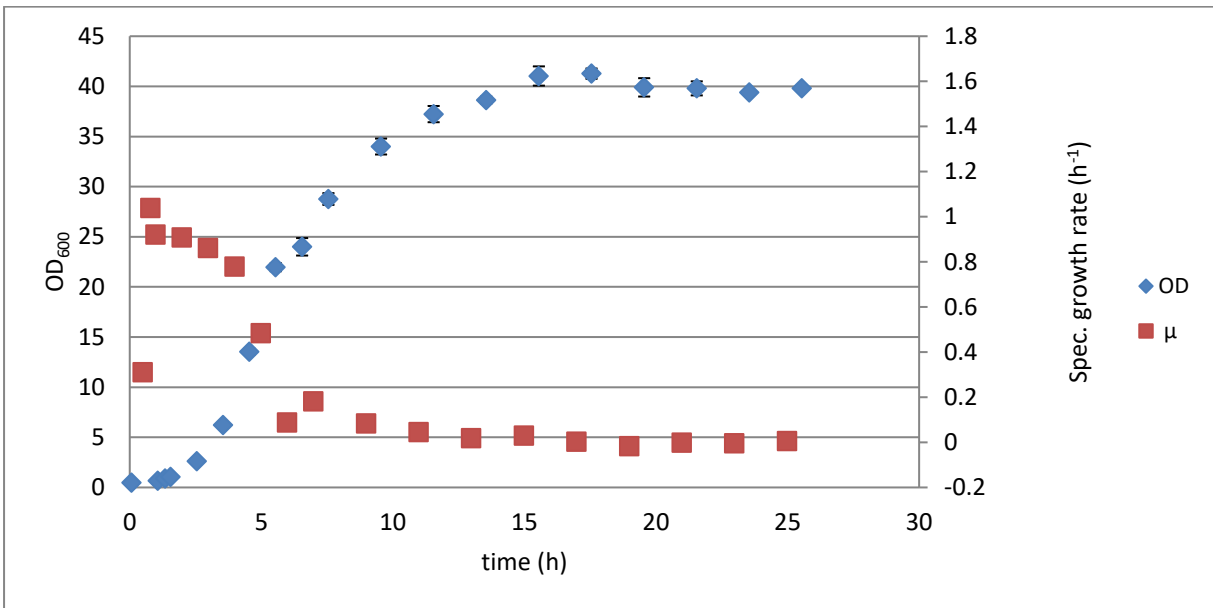
Figure 29. *Specific growth rate (μ) and OD measurements of strain E.coli ΔfhuA pAppA*

By using the equation y = 3.3081x which represents the correlation of cells optical density at 600nm with cell dry weight for the strain *E.coli ΔfhuA* with the coefficient of determination of 0.9966 (Figure 7), cell dry weight has been calculated for the strain *E.coli ΔfhuA pAppA*. Results have been shown in Table 15.

Table 15. *Cell dry weight of a strain E.coli ΔfhuA pAppA*

Time (h)	OD$_{600}$	Cell dry weight (g L^{-1})
0.07	0.48 ± 0.01	0.15 ± 0.00
1.07	0.66 ± 0.00	0.20 ± 0.00
1.35	0.88 ± 0.01	0.27 ± 0.00
1.55	1.06 ± 0.09	0.32 ± 0.03
2.55	2.63 ± 0.10	0.79 ± 0.03
3.55	6.21 ± 0.03	1.88 ± 0.01
4.55	13.53 ± 0.30	4.09 ± 0.09
5.55	21.97 ± 0.40	6.64 ± 0.12
6.55	24 ± 0.87	7.25 ± 0.26
7.55	28.77 ± 0.59	8.70 ± 0.18
9.55	34 ± 0.79	10.28 ± 0.24
11.55	37.23 ± 0.80	11.26 ± 0.24
13.55	38.63 ± 0.35	11.68 ± 0.11
15.55	41.03 ± 0.96	12.40 ± 0.29
17.55	41.27 ± 0.51	12.47 ± 0.16
19.55	39.9 ± 0.92	12.06 ± 0.28
21.55	39.8 ± 0.7	12.03 ± 0.21
23.55	39.4 ± 0.2	11.91 ± 0.06
25.55	39.8 ± 0.17	12.03 ± 0.05

Figure 27 shows bacterial growth curve of strain *E. coli ΔfhuA* pAppA monitored by measuring OD$_{600}$ value. OD$_{600}$ was measured for 24 hours of cultivation after induction when IPTG was added (OD$_{600}$ = 1.06 ± 0.09 at 1.55 h). After reaching maximal OD$_{600}$ value of 41.27 ± 0.51 in sixteenth hour after induction, cells enter stationary phase, remaining OD$_{600}$

value about 40. Percentage of pO_2 and agitator speed during the cultivation are shown in Figure 23.

Dissolved oxygen level rapidly drops in first hours of cultivation (Figure 28) and prior to induction reaches 30 %. Dissolved oxygen level was kept at 30 % of air saturation by controlling the cascading impeller speed. However, percentage of pO_2 can be followed through two peaks around 9 and 15 h where cells have reached the maximal OD_{600} value.

Stirrer speed was up to 950 rpm while cells were in exponential phase. Other cultivation parameters; pH, temperature and overpressure, were kept constant and therefore they are not shown in the charts. Mean value of specific growth rate for strain *E. coli ΔfhuA* pAppA was 0.32 h^{-1}, while generation time was 2.18 h (Figure 29). Maximum specific growth rate was 0.715 h^{-1}. Cell dry weight was up to 12.47 ± 0.16 g L^{-1} at sixteenth hour after induction.

## 4.3.2. Bioreactor cultivation of *Escherichia coli ΔompAompCΔfhuA* pAppA

E. coli ΔompAompCΔfhuA pAppA was cultivated in 5 L bioreactor in TB medium under conditions described before in chapter Batch cultivation. Samples for measuring enzyme activity and determining protein concentration as well as for SDS-page were taken 0, 2, 4, 6, 8, 12, 16, 20 and 24 hours after induction. Enzyme activity and protein concentration were determined in supernatant and in cell lysate.
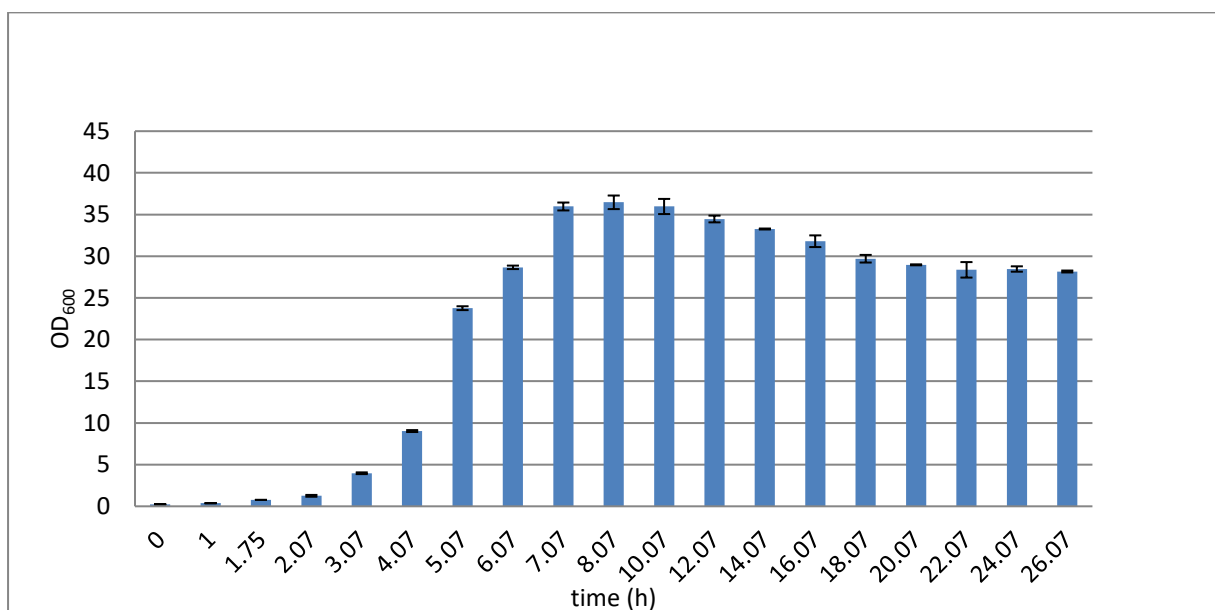
Figure 30. *Growth curve of E. coli ΔompAompCΔfhuA pAppA. Moment of induction was at 2.07 h. N = 1 x 3.*
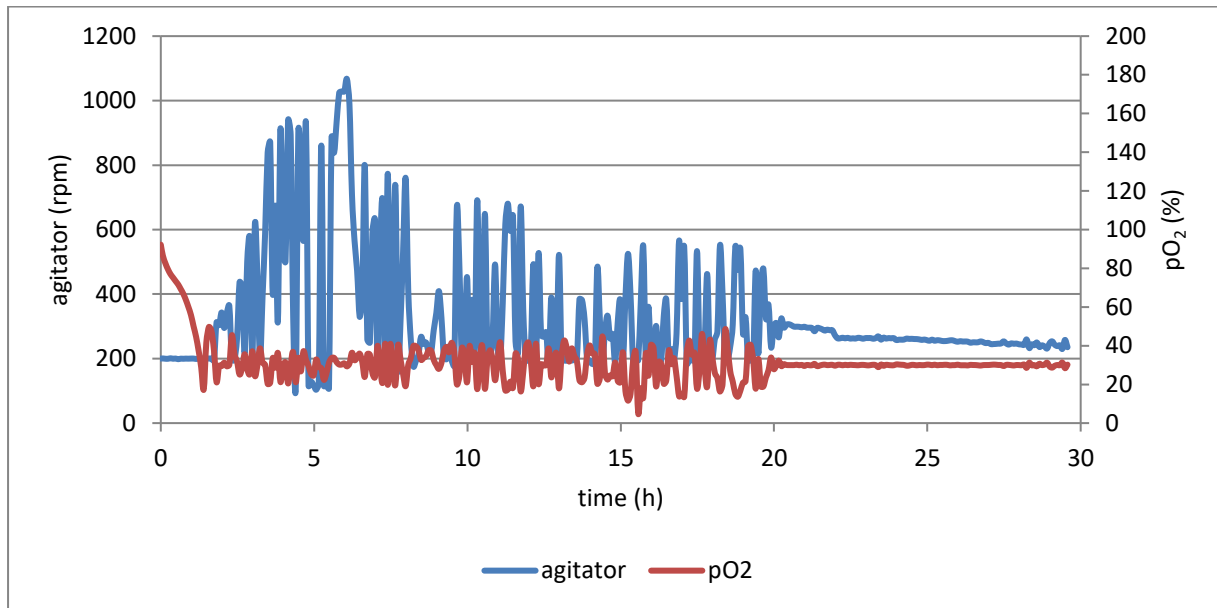
Figure 31. *Parameters of cultivation of E. coli ΔompAompCΔfhuA pAppA*
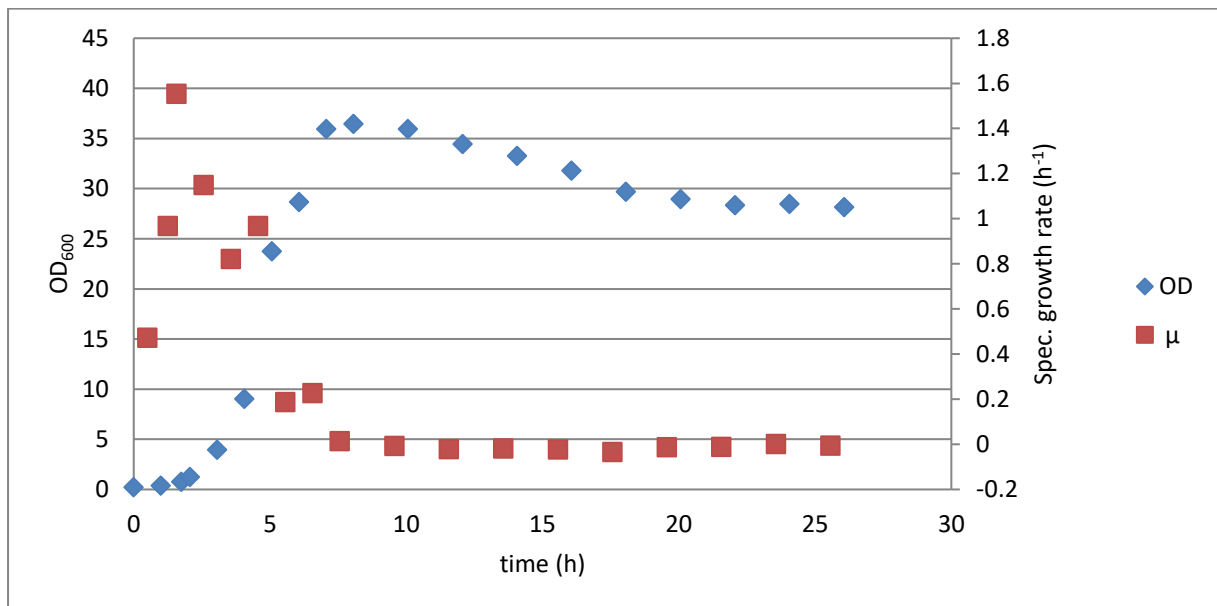
Figure 32. *Specific growth rate (μ) and OD measurements of strain E. coli*
ΔompAompCΔfhuA pAppA

By using the equation y=3.5747x which represents the correlation of cells optical density at
600nm with cell dry weight for the strain *E.coli ΔompAompCΔfhuA* with the coefficient of
determination of 0.9726 (Figure 8), cell dry weight has been calculated for the strain *E.coli*
ΔompAompCΔfhuA pAppA. Results have been shown in Table 16.

Table 16. *Cell dry weight of a strain E.coli ΔompAompCΔfhuA pAppA*

Time (h)	OD_{600}	Cell dry weight (g L^{-1})
0	0.23 ± 0.01	0.06 ± 0.00
1	0.37 ± 0.01	0.10 ± 0.00
1.75	0.77 ±0.01	0.21 ± 0.00
2.07	1.26 ± 0.11	0.35 ± 0.03
3.07	3.97 ± 0.10	1.11 ± 0.03
4.07	9.03 ± 0.12	2.53 ± 0.03
5.07	23.77 ± 0.2	6.65 ± 0.06
6.07	28.67 ± 0.21	8.02 ± 0.06
7.07	35.97 ± 0.47	10.06 ± 0.13
8.07	36.47 ± 0.81	10.20 ± 0.23
10.07	35.97 ± 0.91	10.06 ± 0.26
12.07	34.47 ± 0.40	9.64 ± 0.11
14.07	33.27 ± 0.06	9.31 ± 0.02
16.07	31.8 ± 0.7	8.90 ± 0.20
18.07	29.7 ± 0.46	8.31 ± 0.13
20.07	28.97 ± 0.06	8.10 ± 0.02
22.07	28.37 ± 0.93	7.94 ± 0.26
24.07	28.47 ± 0.32	7.96 ± 0.09

| 26.07	28.17 ± 0.12	7.88 ± 0.03

Figure 30 shows bacterial growth curve of strain *E. coli ΔompAompCΔfhuA* pAppA monitored by measuring OD_{600} value. OD_{600} was measured for 24 hours of cultivation after induction when IPTG was added (OD_{600} = 1.26 ± 0.11 at 2.07 h). After reaching maximal OD_{600} value of 36.47 ± 0.81 in sixth hour after induction, cells enter death phase until 20.07 h of cultivation after which density of the cells remains constant until the end of cultivation (OD_{600} value about 28.5). Figure 31 shows percentage of pO_2 and agitator speed during the cultivation of *E. coli ΔompAompCΔfhuA* pAppA. Dissolved oxygen level was kept at 30 % of air saturation by controlling the cascading impeller speed. Dissolved oxygen level rapidly drops in first hours of cultivation and prior to induction reaches 30 %.

It can be noticed that the highest agitator speed (1067 rpm) was right before cells have reached maximal density. It may be that due to shear stress, on which cells are sensitive due to the weakened cell wall, cells skipped stationary phase and entered death phase immediately.

Mean value of specific growth rate of strain *E. coli ΔompAompCΔfhuA* pAppA was 0.35 h^{-1}, while generation time was 2 h. Cell dry weight was up to 10.20 ± 0.23 g L^{-1} in sixth hour after induction. Maximal specific growth rate was 0.895 h^{-1}.
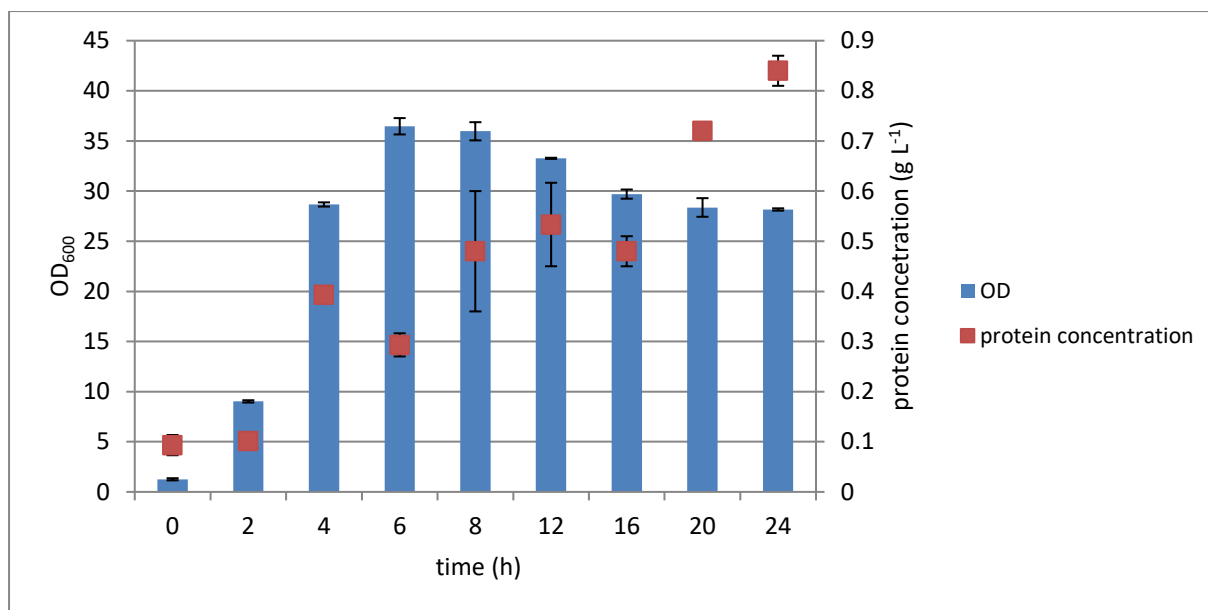
4.3.3. Protein concentration assay

Time points refer to the time after induction point. Results of the protein concentration in cell lysate are now shown.
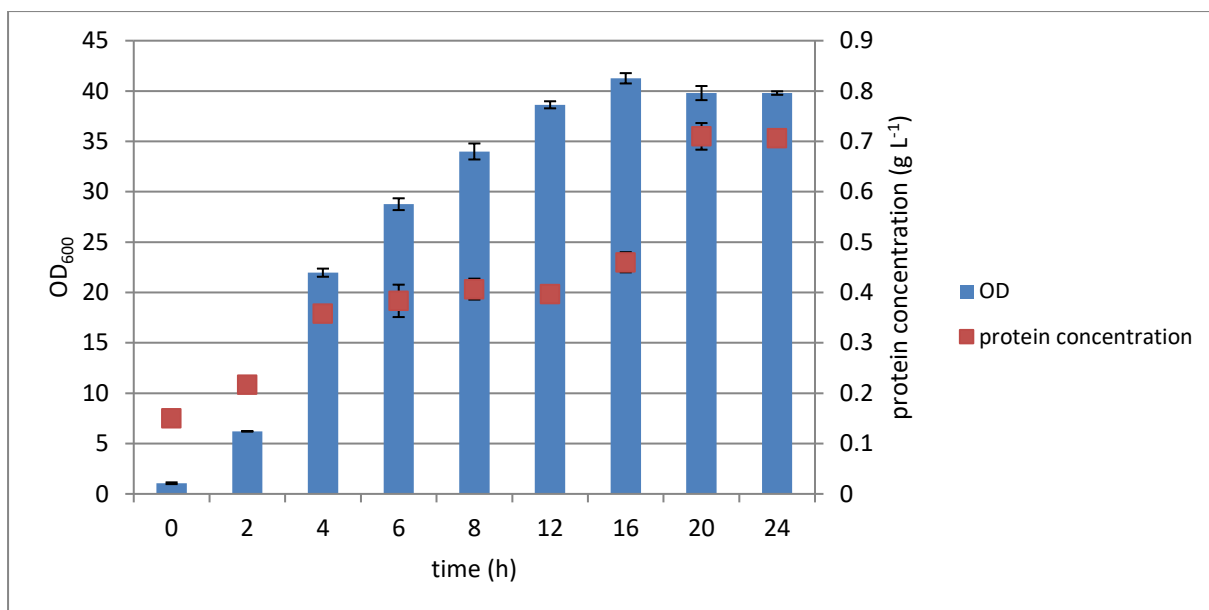
Figure 33. *Optical density and protein concentration in supernatant of E.coli ΔfhuA pAppA.*

Figure 33 shows protein concentration measured in supernatants and OD_{600} of strain *E.coli ΔfhuA pAppA*. Protein concentration in supernatant increases over time what matches the OD_{600}. However, opposite of expectations, in eighth and twelfth hour after induction, protein concentration is quite similar (0.41 ± 0.02 g L^{-1} and 0.40 ± 0.02 g L^{-1}), as well as in twentieth and twenty- fourth hour (0.71 ± 0.03 g L^{-1} and 0.71 ± 0.01 g L^{-1}). Protein concentration in supernatant of strain *E.coli ΔfhuA pAppA* reaches maximal value of 0.71 ± 0.01 g L^{-1} twenty four hours after induction and it is almost five times more than at the point of induction.

Figure 34. *Optical density and protein concentration in supernatant of E. coli ΔompAompCΔfhuA pAppA*

Figure 34 shows protein concentration measured in supernatants and OD_{600} of strain *E. coli ΔompAompCΔfhuA pAppA*. Opposite of expectations, from eight hour until twenty – fourth hour after induction optical density of culture decreases while protein concentration in supernatants increases. Since the protein concentration in sixteenth hour is lower (0.48 ± 0.03 g L^{-1}) than in twelfth hour (0.53 ± 0.08 g L^{-1}) while in twentieth and twenty – fourth hour after induction it is still increasing, it could be that there were some problems either with pipetting or sampling. Protein concentration in fourth hour after induction is higher (0.39 ± 0.01 g L^{-1}) than in sixth hour (0.29 ± 0.02 g L^{-1}) while OD_{600} is still increasing, thus indicating possible problems with pipetting or sampling. Intriguingly, results obtained in *E. coli ΔompAompCΔfhuA pAppA* cultivation in flasks (Figure 15) show as well decrease of optical desnity while protein concentration is increasing and this could be due to the cell lysis.
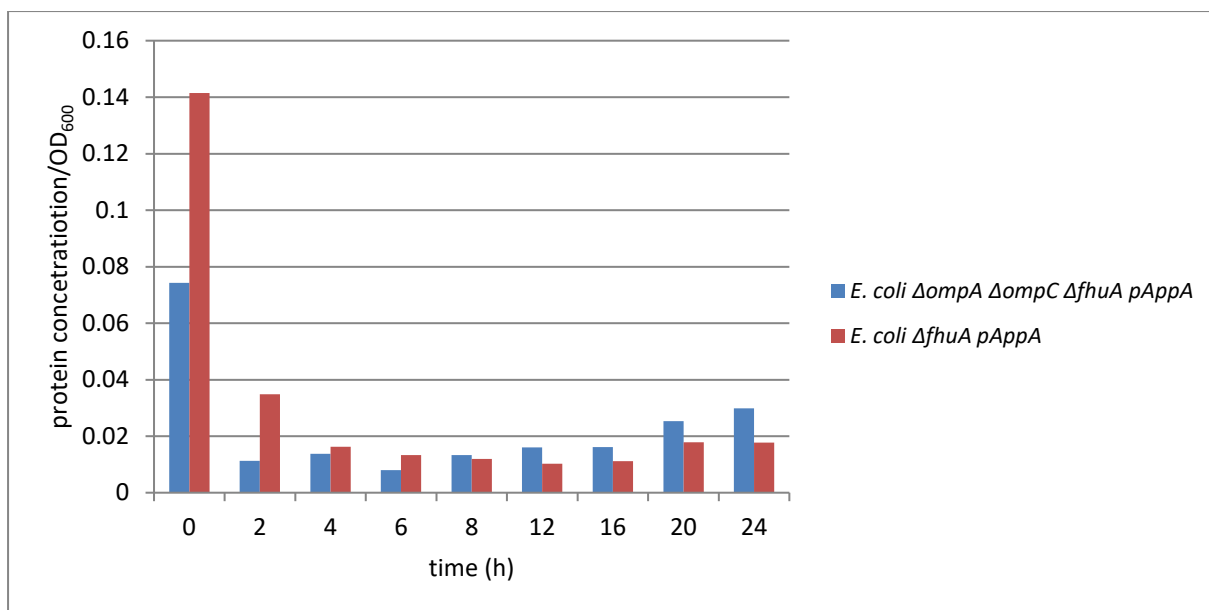
***Figure 35.** Normalized protein concentration comparison in supernatant of two different E. coli strains*

The bars represent the protein concentration in supernatants normalized to the OD_{600} of the respective strains. The highest normalized protein concentration in supernatant of both strains can be noticed at the point of induction. This could be due to the inoculation, since it is possible that lysis of some cells occurred in preculture. At the point of induction, normalized protein concentration of strain *E.coli ΔfhuA pAppA* is two times higher than the normalized protein concentration of strain *E. coli ΔompAompCΔfhuA pAppA*. Normalized protein concentration of *E.coli ΔfhuA pAppA* is higher than *E. coli ΔompAompCΔfhuA pAppA* also in second, fourth, and sixth hour after induction. Eighth hour after induction, the situation is changing in for the benefit of *E. coli ΔompAompCΔfhuA pAppA* compared to normalized protein concentration of *E.coli ΔfhuA pAppA*, but it is important to accentuate that optical density of *E. coli ΔompAompCΔfhuA pAppA* started decreasing in eighth hour of induction.

4.3.4. Enzyme assay results

Table 17 shows enzyme assay results and OD_{600} results for strains cultivated in bioreactor. Table 18 shows volumetric productivity of strains cultivated in bioreactor.

***Table 17.** Enzyme assay and OD_{600} results obtained during bioreactor cultivation*
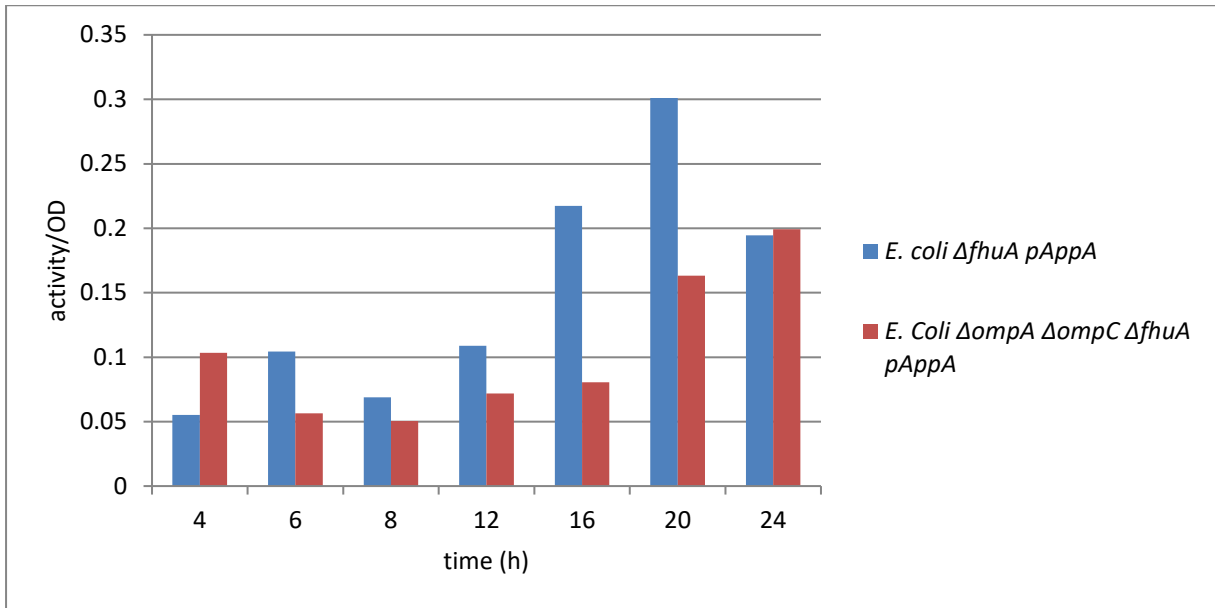
Strain	Time after induction (h)	OD$_{600}$	Total enzyme activity (U mL^{-1})		Normalized enzyme activity (U mL^{-1})	
			supernatant	cell lysate	supernatant	cell lysate
E. coli ΔfhuA pAppA	0	1.06 ± 0.09	-	-	-	-
	2	6.21 ± 0.03	-	0.89 ± 0.08	-	0.143
	4	21.97 ± 0.40	1.22 ± 0.02	2.92 ± 0.06	0.055	0.133
	6	28.77 ± 0.59	3.01 ± 0.08	3.64 ±0.08	0.104	0.127
	8	34.00 ± 0.79	2.34 ± 0.07	6.48 ± 0.29	0.069	0.190
	12	38.63 ± 0.35	4.21 ± 0.05	8.01 ± 0.26	0.109	0.207
	16	41.27 ± 0.51	8.97 ± 0.32	8.90 ± 0.68	0.217	0.216
	20	39.80 ± 0.70	11.98 ± 0.40	9.40 ± 0.63	0.301	0.236
	24	39.80 ± 0.17	7.74 ± 0.18	10.24 ± 0.92	0.194	0.257
E. Coli ΔompA ΔompC ΔfhuA pAppA	0	1.26 ± 0.11	-	-	-	-
	2	9.03 ± 0.12	0.22 ± 0.01	0.53 ± 0.03	0.024	0.059
	4	28.67 ± 0.21	1.57 ± 0.30	3.84 ± 0.20	0.055	0.134
	6	36.47 ± 0.81	2.06 ± 0.18	4.23 ± 0.25	0.057	0.116
	8	35.97 ± 0.91	1.82 ± 0.08	6.19 ± 0.31	0.051	0.172
	12	33.27 ±	2.39 ± 0.08	7.47 ± 0.34	0.072	0.224

			0.06		
16	29.70 ± 0.46	2.39 ± 0.05	6.26 ± 0.15	0.080	0.211
20	28.37 ± 0.93	4.63 ± 0.23	7.65 ± 0.16	0.163	0.270
24	28.17 ± 0.12	5.61 ± 0.27	5.58 ± 0.33	0.199	0.198

Table 18. *Volumetric productivity of strains cultivated in bioreactor*

Strain	Time after induction (h)	Volumetric productivity (U mL^{-1} h^{-1})	
		supernatant	cell lysate
E. coli ΔfhuA pAppA	4	-	1.015
	6	0.895	0.687
	8	0.282	0.931
	12	0.374	0.712
	16	0.646	0.572
	20	0.673	0.473
	24	0.326	0.425
E. Coli ΔompA ΔompC ΔfhuA pAppA	4	0.676	1.654
	6	0.461	0.925
	8	0.267	0.942
	12	0.217	0.693
	16	0.155	0.409
	20	0.245	0.395

	24	0.245	0.229

Figure 36. *Normalized phytase activity in supernatants of E. coli strains ΔfhuA pAppA and ΔompA ΔompC ΔfhuA pAppA cultivated in bioreactor. Time points are for time after induction.*

For the strain *E. coli ΔfhuA* pAppA enzyme activity in the supernatants at the point of induction and second hour after induction as well as in cell lysate at the point of induction could not have been measured due to the too low product concentration. For the strain *E. coli ΔompA ΔompC ΔfhuA pAppA* enzyme activity in the supernatant at the point of induction as well as in cell lysate at the point of induction could not have been measured as well, due to the too low product concentration. It is hard to compare results of enzyme assay during flask cultivation to those obtained during bioreactor cultivation because samples from flask cultivation had too high dilutions, thus eluding the targeted A_{405} that has measuring range from 0.75 – 1.1 where correlation of product concentration and absorbance is linear.

High dilutions of samples affect error values. Although each enzyme activity test is performed the same way, another problem is that the substrate solution is very sensitive to temperature leading to higher readings of absorbance if substrate is not well tempered. Because all of that, there are multiple criteria when it comes to decision which strain shows the best secretion ability.

In supernatant of strain *E. coli ΔfhuA pAppA*, phytase activity increases in sixth hour after induction, after which it decreases in eighth hour after induction. Then, activity increases again and reaches maximal value of 11.98 ± 0.4 U mL^{-1} twenty hours after induction. High enzyme activity in supernatant indicates high protein secretion. Twenty – four hours after induction, phytase activity in supernatant decreases again.

Phytase activity in cell lysate increases over time and reaches maximal value of 10.24 ± 0.92 U mL^{-1} twenty – four hours after induction and it is 11.5x higher than in second hour after induction (Table 17). It is unlikely that maximal value of phytase activity in supernatant of the strain *E. coli ΔfhuA pAppA* is higher than in cell lysate. It could be that with disruption of cells, samples got overheated causing denaturation of some AppA, thus AppA lost part of its total activity.

For the strain *E. coli ΔompA ΔompC ΔfhuA pAppA* phytase activity in supernatant reaches maximum value of 5.61 ± 0.27 U mL^{-1} twenty - four hours after induction. It reaches value more than five times higher than in second hour after induction, suggesting that prolonged time of cultivation increases excreted protein concentration in nutrient medium. It also fits the results of protein concentration in supernatants (Figure 34). Phytase activity in cell lysate had the highest value of 7.65 ± 0.16 U mL^{-1} twenty hours after induction. Compared to the activity in supernatant of strain *E. coli ΔompA ΔompC ΔfhuA pAppA*, total activity in supernatant of strain *E. coli ΔfhuA* pAppA is 3.75 x higher in the sixteenth hour after induction.

If OD$_{600}$ is also included as an important factor of characterization of protein secretion, normalized activity results show that *E. coli ΔfhuA pAppA* remains better secreting (Figure 36) and producing strain (Table 17) because *E. coli ΔfhuA pAppA* reaches up to 2.71 x higher normalized activity in supernatant and 2.42 x higher normalized activity in cell lysate than the *E. coli ΔompA ΔompC ΔfhuA pAppA*.

Volumetric productivity of strain *E. coli ΔfhuA pAppA* has two maximum values both in supernatant and in cell lysate, while on the other hand strain *E. coli ΔompA ΔompC ΔfhuA pApp* has one maximum value both in supernatant and in cell lysate (Table 18). Second maximum value of volumetric productivity of strain *E. coli ΔfhuA pAppA* is a consequence of better cultivation conditions in bioreactor, hence the growth of a strain is more stable even with the smaller growth rate compared to the flask cultivation of strain. The lower robustness

of strain *E. coli ΔompA ΔompC ΔfhuA pAppA* compared to strain *E. coli ΔfhuA pAppA,* has a great impact on cell cultivation in bioreactor, which is why cells skipped stationary phase and entered death phase immediately. Since the robustness of cell influences growth, growth rate and OD_{600}, there is also influence in the volumetric productivity.
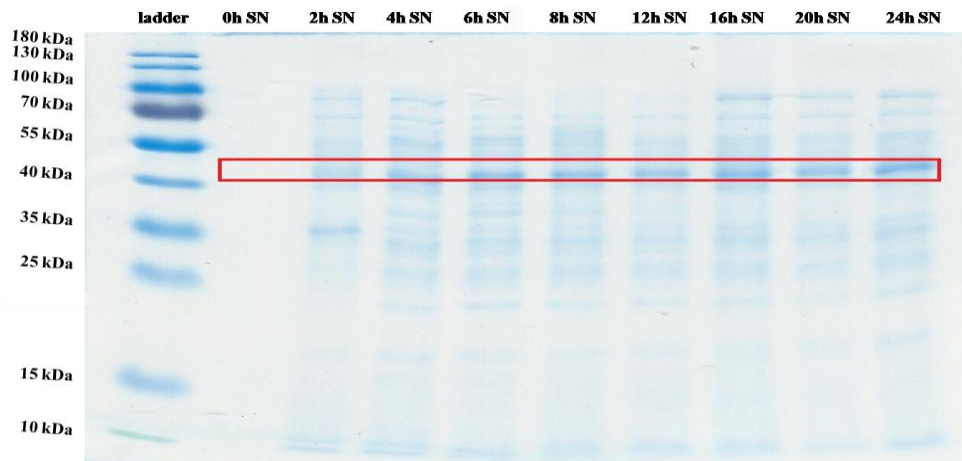
4.3.5. SDS – PAGE
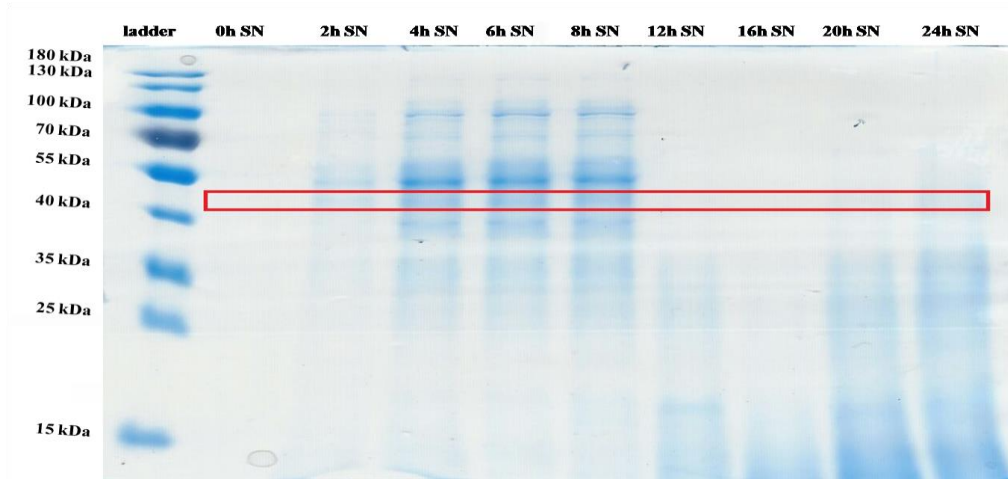
Figure 37. *SDS-PAGE, E.coli ΔfhuA pAppA. 0h, 2h, 4h, 6h, 8h, 12h, 16h, 20h and 24h stand for time after induction samples were taken at. SN stands for supernatant. Red box shows phytase band.*
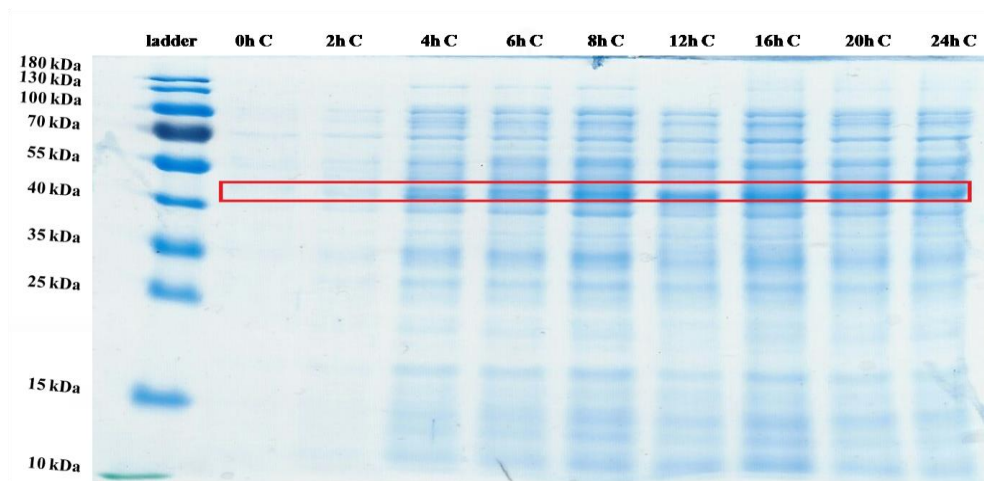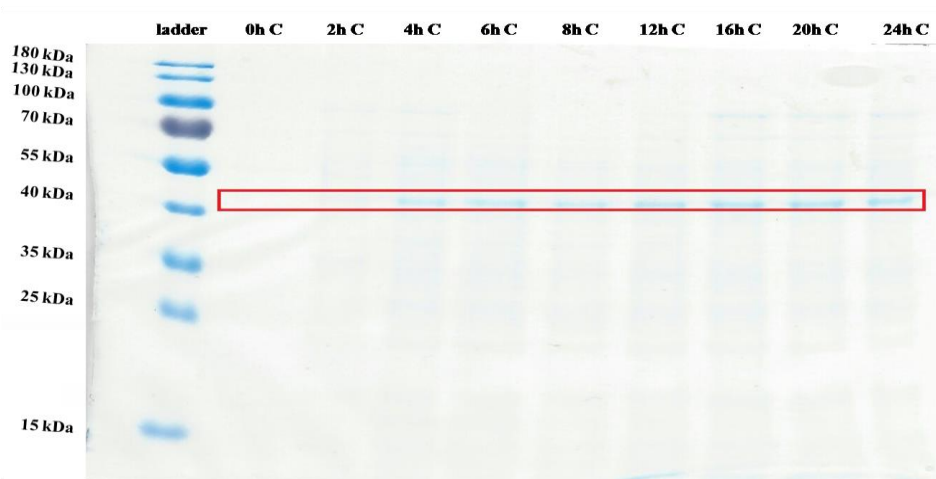

Figure 38. *SDS-PAGE, E.coli ΔfhuA pAppA. 0h, 2h, 4h, 6h, 8h, 12h, 16h, 20h and 24h stand for time after induction samples were taken at. C stands for cell lysate. Red box shows phytase band.*

Figure 39. *SDS-PAGE, E. coli ΔompAompCΔfhuA pAppA. 0h, 2h, 4h, 6h, 8h, 12h, 16h, 20h and 24h stand for time after induction samples were taken at. SN stands for supernatant. Red box shows phytase band.*

Figure 40. *SDS-PAGE, E. coli ΔompAompCΔfhuA pAppA. 0h, 2h, 4h, 6h, 8h, 12h, 16h, 20h and 24h stand for time after induction samples were taken at. C stands for cell lysate. Red box shows phytase band.*

In supernatant samples of strain *E.coli ΔfhuA pAppA* phytase band on SDS-PAGE gel is not visible at the point of the induction, at second hour after induction it is barely visible and in fourth, sixth and eighth hour it is more visible (Figure 37). For the following measuring points it is not visible at all, which does not support results of protein concentration test nor

activity test. Furthermore, it does not match with the SDS-PAGE of the respective strain cultivated in flasks. This result can be a consequence of error that occurred during sample preparation. Because all of that, the experiment should be repeated.

For cell lysate of the reference strain, phytase band could not be seen at the point of the induction, but visibility of phytase band increases over the time in following measuring points (Figure 38) what matches the enzyme assay results where activity of cell lysate is increasing (Table 17).

For samples of protein in supernatants of strain *E. coli ΔompAompCΔfhuA pAppA*, phytase band is not visible at the point of induction, while in following measuring points phytase bands become stronger over the time of cultivation (Figure 39) what supports protein concentration test (Figure 34) and activity assay (Table 17) . For the cell lysate samples of the reference strain, there is no phytase band both at the point of induction and second hour, and in following measuring points phytase bands become stronger over the time of cultivation (Figure 40) what matches with the increasing enzyme activity (Table 17).

5. CONCLUSION AND OUTLOOK

To investigate whether the increased permeability is sufficient to allow secretion of recombinant proteins to an extracellular environment, one single and one triple knock-out mutants of *Escherichia coli* were characterized. Single knock-out *ΔfhuA* pAppA and triple knock-out *ΔompAompCΔfhuA* pAppA were constructed in Laboratory of Fermentation technology and hoped to have increased secretion ability. Firstly, *ΔfhuA* and *ΔompAompCΔfhuA* were cultivated in flasks to have an overview of growth features of both strains. Secondly, *ΔfhuA* and *ΔompAompCΔfhuA* were transformed with plasmid pAppA and phytase AppA was used as a reporter protein. Flask cultivation was carried out to have an overview of features, in terms of growth, protein secretion and enzyme activity. Thirdly, both strains were cultivated in bioreactors over a period of twenty-four hours after induction, again with the aim to characterize them regarding growth, protein secretion and enzyme activity.

1. During the flask cultivation strains *ΔfhuA* and *ΔompAompCΔfhuA* were cultivated. Strain *ΔfhuA* has reached higher maximal measured optical density (30.05±0.41) than *ΔompAompCΔfhuA* (26.58±0.26). Both strains were transformed with plasmid pAppA and cultivated in flasks where once again strain *ΔfhuA* pAppA has reached higher maximal measured optical density (27.21±0.31) than *ΔompAompCΔfhuA* pAppA (15.29±0.42). Extracellular protein concentration was higher for *ΔompAompCΔfhuA* pAppA (0.53±0.05 g L^{-1}) than *ΔfhuA* pAppA (0.39±0.01 g L^{-1}) but it is important to accentuate that high protein concentration in supernatant indicate a good secretion ability of different periplasmic proteins, but also, it can mean cell lysis. The enzyme activity assay results are not reliable as all measured samples of strains had too high dilutions thus eluding a narrow range of linear dependency of absorbance and concentration. Therefore, the enzyme activity assay should be repeated for flask cultivation.

2. Both strains, *ΔfhuA* pAppA and *ΔompAompCΔfhuA* pAppA, were cultivated in bioreactors. Further assessment showed that strain *ΔompAompCΔfhuA* pAppA is more sensitive to shear stress in bioreactor than *ΔfhuA* pAppA, presumably due to lower robustness of the cells caused by weakened cell wall structure since genes encoding for outer membrane proteins have been deleted. *ΔompAompCΔfhuA* pAppA has remained a strain with higher obtained extracellular protein concentration (0.84±0.30

g L^{-1}) than *ΔfhuA* pAppA (0.71 ± 0.01 g L^{-1}). The enzyme activity assay has shown that *ΔfhuA* pAppA is a better secreting and producing strain.

6. BIBLIOGRAPHY

Baba, T., Ara, T., Hasegawa, M., Takai, Y., Okumura, Y., Baba, M., Datsenko, K.A., Tomita, M., Wanner, B.L. and Mori, H. (2006) Construction of *Escherichia coli* K-12 in-frame, single-gene knockout mutants: the Keio collection. *Mol Syst Biol*, **2**, 2006.0008. doi:10.1038/msb4100050

Baslé, A., Rummel, G., Storici, P., Rosenbusch, J.P. and Schirmer, T. (2006) Crystal structure of osmoporin OmpC from *E. coli* at 2.0 A. *J Mol Biol*, **362 (5)**, 933–942.

Batchelor, E., Walthers, D., Kenney, L. J. and Goulian, M. (2005) The *Escherichia coli* CpxA-CpxR envelope stress response system regulates expression of the porins OmpF and OmpC. *J Bacteriol*, **187 (16)**, 5723-5731.

Chatzi, K. E., Frantzeskos Sardis, M., Economou, A. and Karamanou, S. (2014) SecA-mediated targeting and translocation of secretory proteins. *Biochim. Biophys. Acta*, **1843 (8)**, 1466-1474.

Chen, Z.-Y., Cao, J., Xie, L., Li, X.-F., Yu, Z.-H. and Tong, W.-Y. (2014) Construction of leaky strains and extracellular production of exogenous proteins in recombinant *Escherichia coli*. *Microb Biotechnol*, **7 (4)**, 360–370.

Choi, J.H. and Lee, S.Y. (2004) Secretory and extracellular production of recombinant proteins using *Escherichia coli*. *Appl Microbiol Biot*, **64 (5)**, 625–635.

Dassa, E., Tetu, C. and Boquet, P. L. (1980) Identification of the acid phosphatase (optimum pH 2.5) of *Escherichia coli*. *FEBS Lett*, **113**, 68-73.

Dassler, T., Guenter, W. and Schmid, G. (2008) Process for the fermentative production of proteins. No. US20080254511 A1.

Demain, A. L., and Vaishnav, P. (2009) Production of recombinant proteins by microbes and higher organisms. *Biotechnol Adv*, **27 (3)**, 297-306.

Faraldo-Gómez, J. D., Smith, G. R. and Sansom, M. S. P. (2003) Molecular dynamics simulations of the bacterial outer membrane protein FhuA: A comparative study of the ferrichrome-free and bound states. *Biophys. J.*, **85 (3)**, 1406-1420.

Ferguson, A. D., Hofmann, E., Coulton, J. W., Diederichs, K. and Welte, W. (1998) Siderophore-mediated iron transport: crystal structure of FhuA with bound lipopolysaccharide. *Science*, **282 (5397)**, 2215-2220.

Greiner, R., Konietzny, U. and Jany, K.D. (1993) Purification and characterization of two phytases from *Escherichia coli*. *Arch Biochem Biophys*, **303 (1)**, 107–113.

Haefner, S., Knietsch, A., Scholten, E., Braun, J., Lohscheidt, M., Zelder, O. (2005) Biotechnological production and applications of phytases, *Appl Microbiol Biot*, **68 (5)**, 588-597.

Ishida, H., Garcia-Herrero, A. and Vogel, H. J. (2014) The periplasmic domain of *Escherichia coli* outer membrane protein A can undergo a localized temperature dependent structural transition. *Biochim. Biophys. Acta,* **1838(12)**, 3014-3024.

Kleist, S., Miksch, G., Hitzmann, B., Arndt, M., Friehs, K. and Flaschel, E. (2003) Optimization of the extracellular production of a bacterial phytase with *Escherichia coli* by using different fed-batch fermentation strategies. *Appl Microbiol* Biot, **61 (2-6)**, 456–462.

Knoll, A., Bartsch, S., Husemann, B., Engel, P., Schroer, K., Ribeiro, B., Stöckmann, C., Seletzky, J. and Büchs, J.(2007) High cell density cultivation of recombinant yeasts and bacteria under non-pressurized and pressurized conditions in stirred tank bioreactors. *J. Biotechnol*, **132 (2)**, 167-179.

Korz, D. J., Rinas, U., Hellmuth, K., Sanders, E. A. and Deckwer, W. –D. (1995) Simple fed-batch technique for high cell density cultivation of *Escherichia coli*. *J. Biotechnol,* **39 (1)**, 59-65.

Lee, S.Y. (1996) High cell-density culture of *Escherichia coli*. *Trends Biotechnol*, **14 (3)**, 98–105.

Locher, K. P., Rees, B., Koebnik, R., Mitschler, A., Moulinier, L., Rosenbusch, J. P. and Moras, D. (1998) Transmembrane signaling across the ligand-gated FhuA receptor: crystal structures of free and ferrichrome-bound states reveal allosteric changes. *Cell*, **95 (6)**, 771-778.

Masi, M. and Pagès, JM. (2013) Structure, function and regulation of outer membrane proteins involved in drug transport in *Enterobacericeae*: the OmpF/C – TolC Case. *Open Microbiol J.*, **7**, 22-33.

McMorran, L. M., Brockwell, D. J. and Radford, S. E. (2014) Mechanistic studies of the biogenesis and folding of outer membrane proteins in vitro and in vivo: What have we learned to date? *Arch Biochem Biophys*, **564**, 265-280.

Mergulhão, F.J.M., Summers, D.K. and Monteiro, G.A. (2005) Recombinant protein secretion in *Escherichia coli*. *Biotechnol Adv*, **23 (3)**, 177–202.

Miksch, G., Kleist, S., Friehs, K. and Flaschel, E. (2002) Overexpression of the phytase from *Escherichia coli* and its extracellular production in bioreactors. *Appl Microbiol Biot,* **59 (6)**, 685–694.

Misra, R. and Benson, S.A. (1988) Isolation and characterization of OmpC porin mutants with altered pore properties. *J Bacteriol*, **170 (2)**, 528–533.

Mizuno, T., Chou, MY. and Inouye, M. (1983) A comparative study on the genes for three porins of the *Escherichia coli* outer membrane. *J. Biol. Chem.*, **258 (11)**, 6932-6940.

Natale, P., Brüser, T. and Driessen, A.J.M. (2008) Sec- and Tat-mediated protein secretion across the bacterial cytoplasmic membrane--distinct translocases and mechanisms. *Biochim Biophys Acta*, **1778 (9)**, 1735–1756.

Ortiz-Suarez, M., Samsudin, F., Piggot, T. J., Bond, P. J. and Khalid, S. (2016) Full-length OmpA: structure, function, and membrane interactions predicted by molecular dynamics simulations. *Biophys. J.* **111(8)**, 1692-1702.

Pandey, A., Szakacs, G., Soccol, C. R., Rodriguez-Leon, J. A. and Soccol, V. T. (2001) Production, purification and properties of microbial phytases, *Bioresour. Technol,* **77 (3)**, 203-214.

Patel, R., Smith, S. M. and Robinson, C. (2014) Protein transport by the bacterial Tat pathway. *Biochim. Biophys. Acta*, **1843 (8)**, 1620-1628.

Riesenberg, D. (1991) High-cell-density cultivation of *Escherichia coli*. *Curr Opin Biotech,* **2 (3)**, 380-384.

Robinson, C., Matos, C. F. R. O., Beck, D., Ren, C., Lawrence, J., Vasisht, N. and Mendel, S. (2011) Transport and proofreading of proteins by the twin-arginine translocation (Tat) system in bacteria. *Biochim. Biophys. Acta*, **1808 (3)**, 876-884.

Rosano, G.L. and Ceccarelli, E.A. (2014) Recombinant protein expression in *Escherichia coli*: advances and challenges. *Front Microbiol*, **5**, 172.

Ruiz, N., Kahne, D. and Silhavy, T. (2006) Advances in understanding bacterial outer-membrane biogenesis. *Nat. Rev. Microbiol.*, **4**, 57-66.

Sandkvist, M. and Bagdasarian, M. (1996) Secretion of recombinant proteins by Gram-negative bacteria. *Curr Opin Biotech*, **7 (5)**, 505-511.

Shokri, A., Sandén, A. M. and Larsson, G. (2003) Cell and process design for targeting of recombinant protein into culture medium of *Escherichia coli*. *Appl Microbiol Biotechnol*, **60 (6)**, 654-664.

Wang, Y. (2002) The function of OmpA in *Escherichia coli*. *Biochem Bioph Res Co*, **292 (2)**, 396–401.

Wich, G. and Dassler, T. (2008) Process for the fermentative production of antibodies. No. US20080206818 A1.

Yoon, S., Kim, S. and Kim, J. (2010) Secretory Production of Recombinant Proteins in *Escherichia coli*. *Rec Pat Biotechnol*, **4 (1)**, 23–29.
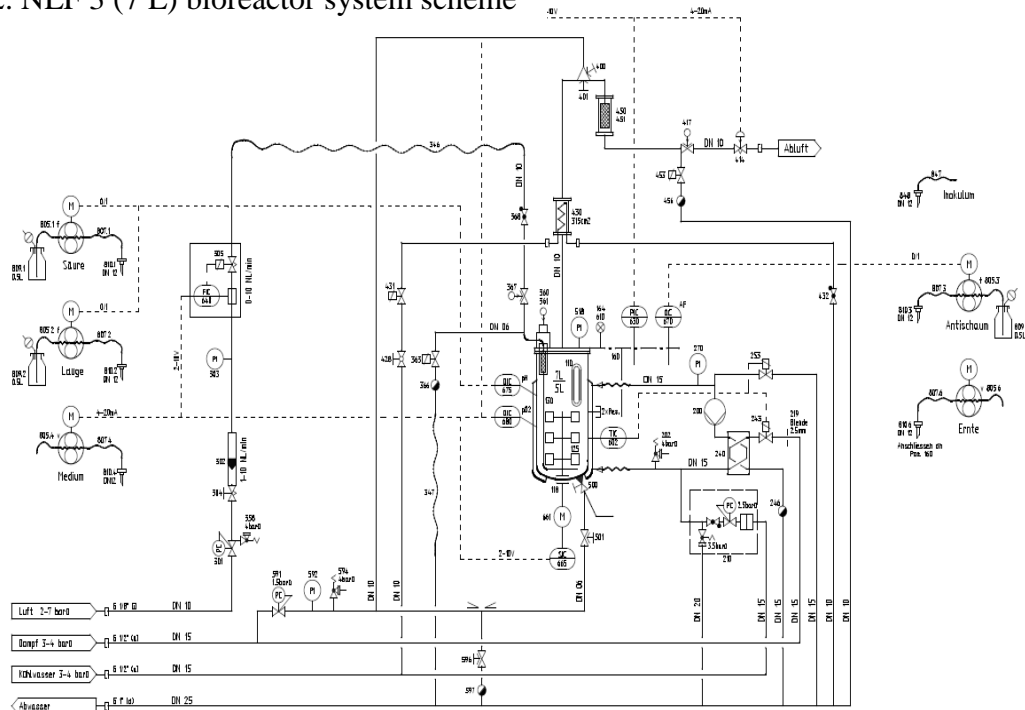
7. **APPENDIX**

1. Bioreactors specifications

Bioreactor model	Bioengineering NLF 3
Process control	BioSCADA Bioengineering
Total volume	7 L
Reactor diameter (D)	155 mm
Reactor height (H)	360 mm
Impeller diameter (d)	60 mm
Impeller blade width (a)	21 mm
Impeller blade height (b)	16 mm
Blade diameter (c)	30 mm
Number of blades	6
Number of stirrer levels	3
Blade bottom and bioreactor bottom distance	70 mm
Distance between two stirrers (k)	122 mm
Distance between the 2nd stirrer and bioreactor bottom	ca. 65 mm
Stirrer blade and air opening	ca.60 mm
Stirring shafts diameter	12 mm
Number of baffles	4
Baffle height (g)	326 mm
Baffle width (e)	15 mm
Baffle and bioreactor wall distance (f)	3 mm
Baffle and bioreactor bottom distance (h)	0 mm
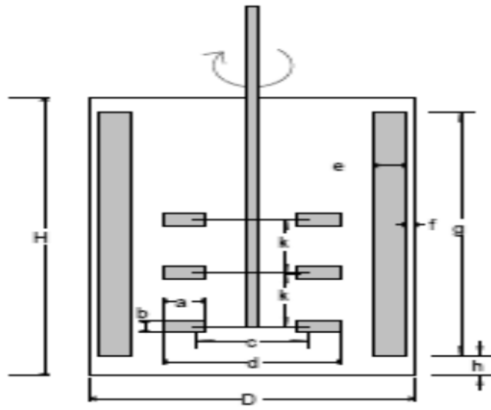
2. NLF 3 (7 L) bioreactor system scheme